Politecnico di Torino
Master degree of Physics of Complex Systems
Master Degree Thesis

Clusters and shocks in a Totally Asymmetric Simple Exclusion Process with interactions

Politecnico
di Torino

Supervisor:
Alessandro Pelizzola
Marco Pretti

Candidate:
Giacomo Accornero

Academic year 2024/2025

Contents

1 Introduction

The Totally Asymmetric Simple Exclusion Process (TASEP) is the simplest version of a class of stochastic models proposed in 1968-69 [[5, 6]] to describe the kinetics of protein synthesis on mRNA, related to the stochastic motion of molecular motors on a track. Over the year, this simple model has inspired many studies of nonequilibrium phenomena, becoming with its variants a paradigmatic model in nonequilibrium statistical physics. This model is usually defined on a linear chain, where each site can be occupied by at most one particle , and each particle can hop in a selected direction to the adjacent site, provided the latter is empty, with a rate whose specific value depends on the model definition.

The aim of this thesis is to study the behavior of one variant of this model, i.e. considering nearest-neighbor (NN) interactions which affect the hopping rates, following [1, 2]. In [1], Mina et al develop the analytical Pair Approximation (PA) theory to describe the steady state of the TASEP with Nearest-Neighbor interactions, for which it is known to be exact. In [2], Hao et al consider a simple version of the NN TASEP model, known as the Facilitated Model (FM), in which they assume the interaction of the particle that is hopping only with a particle in the previous site along the direction of motion. In particular, they study the behavior of the length of clusters in the steady state of this model and they also find the presence, in a numerical way, of a critical density where this behavior changes. Here, we will find an analytical expression of the cluster length distribution and of the critical density using the PA theory. We also confirm the existence of this critical density for a model (related to FM by a Symmetry) known as Antal-Schütz (AS) Model, in which we consider the interaction of the particle that is hopping with the subsequent site. Also, we try to understand the transient behavior of the two models, starting from an initial condition with two bulk regions of different density, until the system relaxes into a uniform steady state. To this end, we numerically integrate the dynamical equations of the PA theory and we compare the solution with the results obtained from numerical simulations.

The thesis is structured in this way:

- In chapter 2 we describe the TASEP with NN interactions and the two particular cases introduced before, the Facilitated Model and the Antal-Schütz model.

- In Chapter 3 we introduce the analytical Pair Approximation theory, developed in [1], and we discuss in detail the equations for the density, the correlation and the current that characterize the behavior of our model.

- In Chapter 4 we explain the Gillespie algorithm, which we use to perform the numerical simulations of the model.

- In Chapter 5 we present the results we have found for the Facilitated Model both for the steady state, in particular the behavior of the length of the clusters, and for the transient behavior, in which we explain the dynamics of the shocks analyzing the evolution of the density, correlation and of the current.

- In chapter 6 we explain the results obtained for the Antal-Schütz Model, emphasizing the symmetry which relates it to the FM.

- In chapter 7 we summarize the results obtained in the two models.

2 Model

The model we consider is defined on a linear chain of L sites, labeled by $i = 1, ..., L$.

For each site, we introduce an occupation state variable σ_i that is $\sigma_i = 1$ if the site is occupied and $\sigma_i = 0$ if not occupied, reflecting the fact that each site can be occupied by at most one particle under the hard-core exclusion effect.

According to the usual definition of the TASEP, each particle can hop only in one direction when the adjacent site is not occupied, and we choose Periodic Boundary Conditions (PBCs), so the particle in the last site hops in the first one if possible. The particle hopping rate, following [1] and [2], depends on the Nearest Neighbor (NN) interaction. In general, the hopping rate can take four different values, depending on the occupation of the site after the one where the particle arrives and before the site in which the hop takes place. Denoting by $w_i[\sigma_{i-1},\ \sigma_i,\ \sigma_{i+1},\ \sigma_{i+2}]$ the hopping rate in site i, we define:

$$w_i[0, 1, 0, 0] = p \tag{2.0.1}$$

$$w_i[0, 1, 0, 1] = q \tag{2.0.2}$$

$$w_i[1, 1, 0, 0] = r \tag{2.0.3}$$

$$w_i[1, 1, 0, 1] = s \tag{2.0.4}$$

In this terms we are going to study two different cases, defined by particular choices of the hopping rates:

1. Facilitated model : the particle in site i interacts with the one in site $i - 1$.

2. Antal-Schütz model: the particle in site i interacts with the one in site $i + 2$.

As we can see in table 1, in each model the hopping rate can take only 2 different values, since the Facilitated (respectively Antal-Schütz) Model does not depend on σ_{i+2} (resp. σ_{i-1}). So we obtain in Facilitated model:

$$p = q = e^{-\beta E} \tag{2.0.5}$$

and

$$r = s = e^{\beta E} \tag{2.0.6}$$

rate symbols	$i-1$	i	$i+1$	$i+2$	FM rate	AS rate
p		•			$e^{-\beta E}$	$e^{-\beta E}$
r	•	•			$e^{\beta E}$	$e^{-\beta E}$
q		•		•	$e^{-\beta E}$	$e^{\beta E}$
s	•	•		•	$e^{\beta E}$	$e^{\beta E}$

Table 1: In the first column we have the symbols of the different case, in the subsequent 4 column of the table we have the visual representation of the different case, while in the last two we have the rate for the two different model

In the Antal-Schütz model case we find:

$$p = r = e^{-\beta E} \tag{2.0.7}$$

and

$$q = s = e^{+\beta E} \tag{2.0.8}$$

as usual $\beta = (k_B T)^{-1}$, where k_B is the usual Boltzmann constant and T is the thermodynamic temperature. In this thesis we set $\beta = 2$, following a case of [2]. All hopping rates have been written as functions of the energy interaction between the nearest neighbors that, in general, can vary from $-\infty$ to $+\infty$. To simplify this range, we can introduce an interaction parameter θ, defined as:

$$\theta = \frac{e^{\beta E}}{e^{\beta E} + e^{-\beta E}} \tag{2.0.9}$$

With this definition, the interaction parameter θ vary from 0 to 1, simplifying our discussion.

Indeed, we can defined the energy interaction in function of θ:

$$E(\theta) = \frac{1}{\beta} \ln \sqrt{\frac{\theta}{(1-\theta)}} \tag{2.0.10}$$

such that our model depends only on the interaction parameters θ and in the mean density ρ.

Different values of θ correspond to different types of interaction:

$\theta < 0.5$: It implies $E < 0$, in the Facilitated model we have an attractive interaction, while in the Antal-Schütz model we have a repulsive interaction.

$\theta = 0.5$:It implies $E = 0$, so we recover the simple TASEP model, because we do not have interaction.

$\theta > 0.5$:It implies $E > 0$, in the Facilitated model we have an repulsive interaction, while in the Antal-Schütz model we have a attractive interaction.

In the Facilitated model an attractive interaction means that a particle is less likely to hop if there is a particle before it, while the repulsive regime means that a particle is more likely to hop because it is repelled by a particle in the previous site. In the Antal-Schütz model an attractive interaction means that a particle is more likely to hop to a site adjacent to a subsequent particle and a repulsive interaction means that a particle in the same condition will be less likely to hop. From table 1, we can also observe the presence of a particle-hole symmetry between the two model. Indeed, we can see that:

$$\begin{aligned} w_i^{FM}[\sigma_{i-1},\ \sigma_i,\ \sigma_{i+1},\ \sigma_{i+2}; E(\theta)] = \\ = w_i^{AS}[1-\sigma_{i+2},\ 1-\sigma_{i+1},\ 1-\sigma_i,\ 1-\sigma_{i-1}; E(1-\theta)] \end{aligned} \tag{2.0.11}$$

Therefore, the Antal-Schütz Model can be map to the Facilitated model performing a changing of variable on the two quantity that determine the model, i.e. ρ and θ, performing the change $(\sigma_i, \theta) \Rightarrow (1-\sigma_i, 1-\theta)\ \forall i$ and also invert all the indices of site as we have the hopping toward left. The reason of the change of variable in the interaction parameter can be understood performing it in eq. (2.0.10), obtaining:

$$E(1-\theta) = -E(\theta) \tag{2.0.12}$$

This symmetry is present both in the steady state and in the transition behavior of the model as we can see in section 6.

In the next section we are going to illustrate the PA theory, developed in [1], with which we will study the two models. Results from the PA theory will be compared to numerical simulations in section 5 and in section 6.

3 Analytical methods

Let us now present the PA theory in the most general case. First of all, we define the marginal distributions and expectation values. We denote the marginal distribution at time t, for a cluster of consecutive nodes starting at i, by

$$P_i^t[klm...] = \mathbb{P}[\sigma_i^t = k, \sigma_{i+1}^t = l, \sigma_{i+2}^t = m, ...] \tag{3.0.1}$$

Moreover, we define specific symbols for the local densities and NN correlations, respectively:

$$\rho_i^t = \langle \sigma_i^t \rangle \tag{3.0.2}$$

$$\phi_i^t = \langle \sigma_i^t \sigma_{i+1}^t \rangle \tag{3.0.3}$$

As we are dealing with binary random variables, the latter quantities completely specify 1-node and 2-node marginals (for NN pairs), which can be used to parameterize them as follows:

$$P_i^t[1] = \rho_i^t \tag{3.0.4}$$

$$P_i^t[0] = 1 - \rho_i^t \tag{3.0.5}$$

And for the two-node marginals:

$$P_i^t[11] = \phi_i^t \tag{3.0.6}$$

$$P_i^t[10] = \rho_i^t - \phi_i^t \tag{3.0.7}$$

$$P_i^t[01] = \rho_{i+1}^t - \phi_i^t \tag{3.0.8}$$

$$P_i^t[00] = 1 - \rho_i^t - \rho_{i+1}^t + \phi_i^t \tag{3.0.9}$$

Now we want to evaluate the time evolution of the ρ_i^t and ϕ_i^t. To do this, we follow the derivation from the master equation developed in [1].

They obtain a typical continuity equation for the local density:

$$\dot{\rho_i^t} = J_{i-1}^t - J_i^t \tag{3.0.10}$$

where J_i^t represents the probability current from i to $i+1$ at time t.

This current can be written as a sum of 4 contributions, one for each possible combination of backward and forward occupation states, in formula:

$$J_i^t = J_i^t(0,0) + J_i^t(0,1) + J_i^t(1,0) + J_i^t(1,1) \tag{3.0.11}$$

where

$$J_i^t(k,n) = w_i(k,1,0,n)P_{i-1}^t[k10n] \tag{3.0.12}$$

Regarding local correlations, we have the following equation:

$$\dot{\phi}_i^t = J_{i-1}^t(0,1) + J_{i-1}^t(1,1) - J_{i+1}^t(1,0) - J_{i+1}^t(1,1) \tag{3.0.13}$$

In the end, we can see that the time-derivatives of ρ_i and ϕ_i can be written in terms of 4-node marginals, so the resulting time-evolution equations, though exact, are not closed.

So, they apply the Bethe approximation to deal with the closure for the probability for the four sites:

$$P_i^t[k10n] \cong \frac{P_i^t[k1]P_{i+1}^t[10]P_{i+2}^t[0n]}{P_{i+1}^t[1]P_{i+2}^t[0]} \tag{3.0.14}$$

Considering the steady state, we drop the time index in all the equations, and we set the derivative at zero in eq. (3.0.13) and in eq. (3.0.10). Setting eq. (3.0.10) to zero, means that the current $J_i = J$ for all sites, implying a spatial homogeneity of the current of the model. Taking again eq. (3.0.10), we have that now the LHS of this equation does not depends on the space so also the RHS have not to depend on it, that implies that we have spatial homogeneity also for the density.

After this we can introduce a new quantity, as [1] did:

$$\eta = \frac{P[10]}{P[1]P[0]} = \frac{\rho - \phi}{I} \tag{3.0.15}$$

where I is defined as

$$I = \rho(1-\rho) \tag{3.0.16}$$

Following the calculation performed in [1] we can find an expression for η.

$$\frac{1}{\eta} = \frac{1 + \sqrt{1 - 4(1-\nu^2)I}}{2} \tag{3.0.17}$$

where ν is defined as

$$\nu = \sqrt{\frac{q}{r}} \tag{3.0.18}$$

In the case of Facilitated Model ν takes the values $e^{-\beta E}$, while in Antal-Schütz takes the values $e^{\beta E}$.

Fitting eq. (3.0.15) in this equation, we find an expression for ϕ which depends only on ρ:

$$\phi = \rho - \frac{2\rho(1-\rho)}{1+\sqrt{1-4(1-\nu^2)I}} \tag{3.0.19}$$

In the next section, we are going to illustrate the algorithm used in the numerical simulations.

4 Simulation methods

In order to obtain numerical results for our model, we use the well known Gillespie Algorithm. This algorithm is also called Kinetic Montecarlo method and it's a very efficient technique to simulate this kind of model.

4.1 Gillespie Algorithm

The Stochastic Simulation Algorithm developed by Gillespie is a Monte Carlo technique to simulate continuous time Markov processes. The main idea is to draw at random both the time of the next transition and which of the possible states is taken: for each pair of generated random numbers a new state is selected, this is a direct generation method with 100% efficiency.

It achieves this by calculating the probability of each possible transition occurring within a given time interval and then randomly selecting which one will occur next.The algorithm proceeds as follows:

1. Initialization: Define the initial state of the system, specifying the number of particles. Determine the set of possible transition that can occur and their associated rate constants.

2. Calculation of Rates: For each action we calculate its rate w_i

3. Calculating the Time to the Next Transition: The time until the next transition occurs, τ, is a random variable drawn from an exponential distribution with a parameter that is the sum of all rates w_i:

$$w_0 = \sum_{i=1}^{M} w_i \tag{4.1.1}$$

   where M is the total number of transition. This time τ is calculated as:

$$\tau = \frac{1}{w_0} ln(\frac{1}{r_1}) \tag{4.1.2}$$

   where r_1 is a random number drawn from a uniform distribution between 0 and 1.

4. Selecting the transition to occur: The specific transition in position i that will occur is chosen probabilistically based on the rate. A second

random number, r_2, is drawn from a uniform distribution between 0 and 1. The transition i is selected such that:

$$\sum_{j=1}^{i-1} w_j < r_2 w_0 \leq \sum_{j=1}^{i} w_i \tag{4.1.3}$$

5. Updating the system state: The state of the system is updated to reflect the occurrence of the selected transition.

6. Iteration: Steps 2-5 are repeated until a desired simulation time is reached or a specific condition is met.

We use an exponential queue R to reorder all possible transition from the most probable to the least one.

For the first step, we look at the occupation vector $\vec{\sigma}$ and every time we find a possible transition, we insert into our R the position in which it can occur and the relative rate.

Due to the implementation of the Exponential Queue in a package of Julia, i.e. CavityTools.jl, developed in [4] , every time we insert one of these transitions, Steps 2, 3 and 4 are already done automatically.

For step 5, we take the position chosen and we perform the hop of our particle setting $\sigma_i = 0$ and $\sigma_{i+1} = 1$ and we also have to update the rate's exponential queue in the position corresponding to the hop and check whether any rates has changed or any new transition can occur,i.e. after the transition we can have that the particle that has hopped in site $i+1$ can perform another hopping if $\sigma_{i+2} = 0$, so we have to check the neighbor of $i + 2$ and insert in the exponential queue this new possible transition with the corresponding rate.

When we studying the steady state of our model, such that we can check how much accurate are the prediction of the theory with respect to the simulations, we first initialize with some selected density and we simulate it until we reach the steady state, using the current as our checking variable, i.e. once the autocorrelation of the current are approximately zero, the system has reach the steady state and we can start to perform the measure, as we can see in section 5.1. Conversely, to studying the transient behavior, we are going to perform a large number N of realization of the model and mediate the results obtained for all of them to generalize our results, as we can see in section 5.2.

In the next sections, we are going to illustrate the results obtained for the two different models.

5 Facilitated Model

In this section, we are going to illustrate the various results we found in the Facilitated model.

We start describing the steady state and its properties concerning the cluster size and, after this, we analyze the transient behavior of our model. The transient behavior obtained integrating the equation obtained by the PA theory mimics quite well the behavior simulate with our algorithms, as we will see in section 5.2.

We find that the numerical simulations coincides with the PA theory at the steady state, as we can see in section 5.1.

5.1 Steady state

To study the steady state, we initialize our variable $\vec{\sigma}$ with a defined configuration such that our system has a precise density.

As we define before $\vec{\sigma}$, introducing a particle in a random site i of our model correspond to set at 1 the corresponding σ_i. To recreate a desiderate density in our model, we introduce an amount of particle in our model, such that the fraction of this number of particles divide by the size of this system is our chosen density, and this coincides with setting at 1 the same amount of σ_i, with i choose randomly in the set of free site, i.e. $\vec{\sigma} : \sigma_i = 0$.

After this we let the system evolve until it reaches the stationarity, using the current as our check variable, i.e. we have reach the steady state when it stabilize to a precise value in all the site of our model, that is given by eq. (5.2.2). So, once reaching it, we can start to perform our measures of the length of cluster that can form in our model as [2] find in their study.

5.1.1 Cluster's length

We study the probability of cluster's length, where the clusters are defined as group of particles that occupy consecutive site, to see if there are some significant behaviors depending on the regime we consider. For the theoretical part, we use eq. (3.0.19) and we introduce a variable:

$$z = \frac{\phi}{\rho} \tag{5.1.1}$$

that describe the conditional probability of having a particle in site $i + 1$ knowing that there is a particle in site i.

The probability of a chosen particle to belong to a cluster of length l is:

$$p(l) = (1-z)^2 l z^{l-1} \tag{5.1.2}$$

where z^{l-1} is the probability of having l subsequent particle, $(1-z)^2$ is the probability of not having a particle in before and after the two extremes of the cluster and, finally, we have to multiplicate by l because we can choose among all of the particles that form the cluster.

In order to develop the numerical simulation, once we reach the steady state, we make 300 measurements of the probability of cluster's length. To do so for every measurement, we check the size of every cluster present in that moment putting in an array that tell us how many cluster of a precise length are present, weighted by the size of the system, i. e. in this array in position 2 we have the number of cluster of length 2 present. Now, after each transition, we check the size of the clusters in our model and, for each size found, we record this numbers. At the end of the procedure, we have an array that tell us the multiplicity of every possible length of cluster, i.e. at the position 1 of this vector we have the numbers of times we have a cluster of length 1 in our model. Now, we divide by the total number of the simulations, therefore, we obtain the probability of the cluster's length on this realization.

So, we perform the calculation and the simulations for the three different regimes defined in section 2: $\theta = 0.2$ for attraction, $\theta = 0.5$ in which we have no interaction, so we recover the pure TASEP, $\theta = 0.8$ for repulsion. First of all in fig. 1, fig. 2 and in fig. 3, we find good agreement between the theoretical result and the numerical one, confirming the result that the PA theory is exact for this model. Second, for every regime, we vary the mean density, selecting three different values, i.e. one for low density, $\rho = 0.2$, one at half filling of our system, $\rho = 0.5$, and one for high density, $\rho = 0.8$.

We find that, the probability of length of cluster has a monotonic behavior for small density and non-monotonic for large density, while for half filling of our system we see a change of the behavior from a non-monotonic one in fig. 1 and fig. 2 to a monotonic one in fig. 3. So, this suggests the presence of a critical density, depending on the interaction parameter θ, for which we have this change of behavior and we will see in detail in the next subsection.

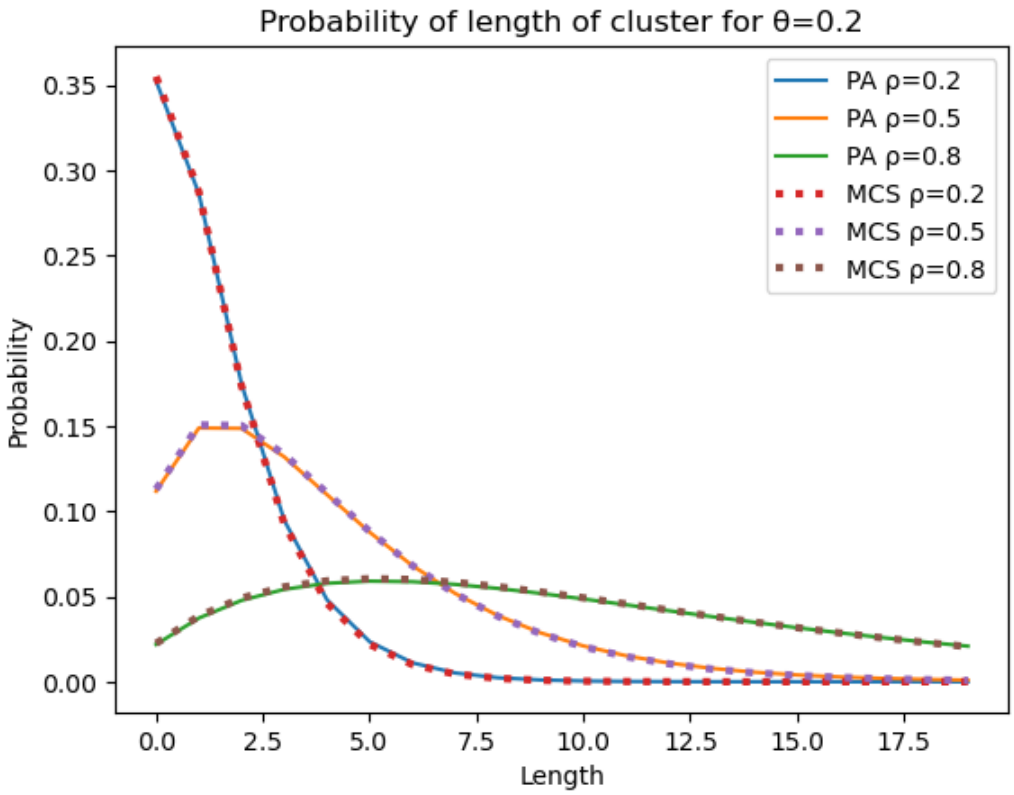

Figure 1: Probability of length of cluster for attractive regime, $\theta = 0.2$.In solid line we have the results obtained with the theory, while in dot line we have the results obtained by numerical simulations.

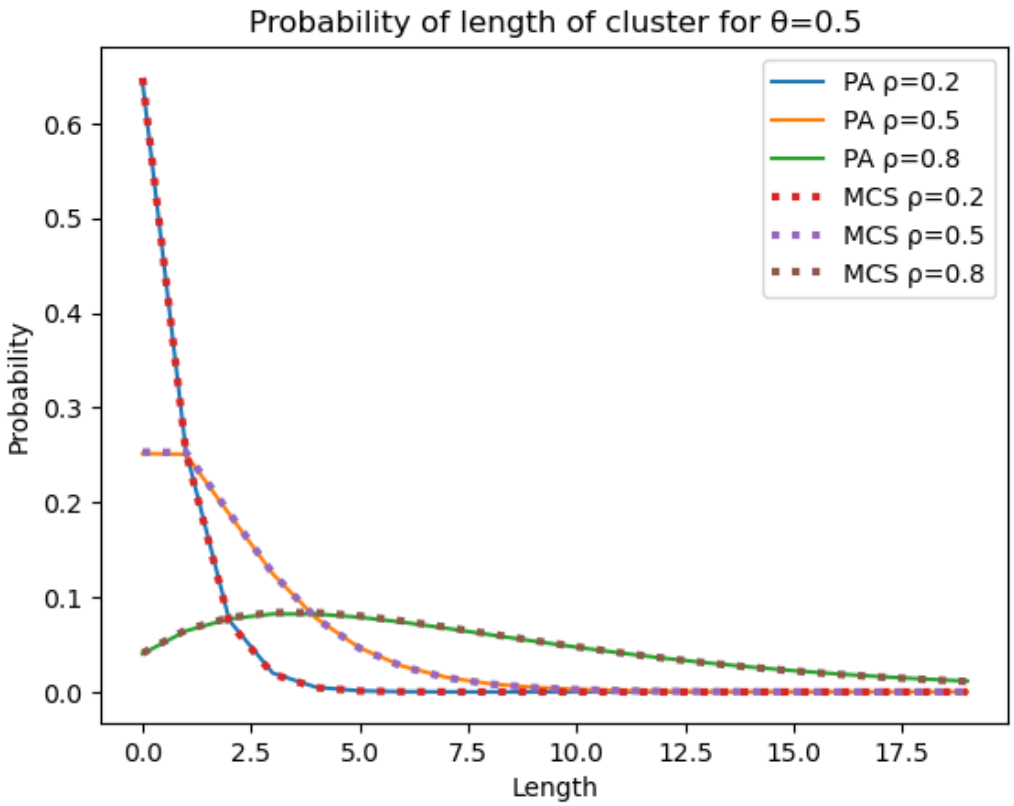

Figure 2: Probability of length of cluster for pure TASEP, $\theta = 0.5$.In solid line we have the results obtained with the theory, while in dot line we have the results obtained by numerical simulations

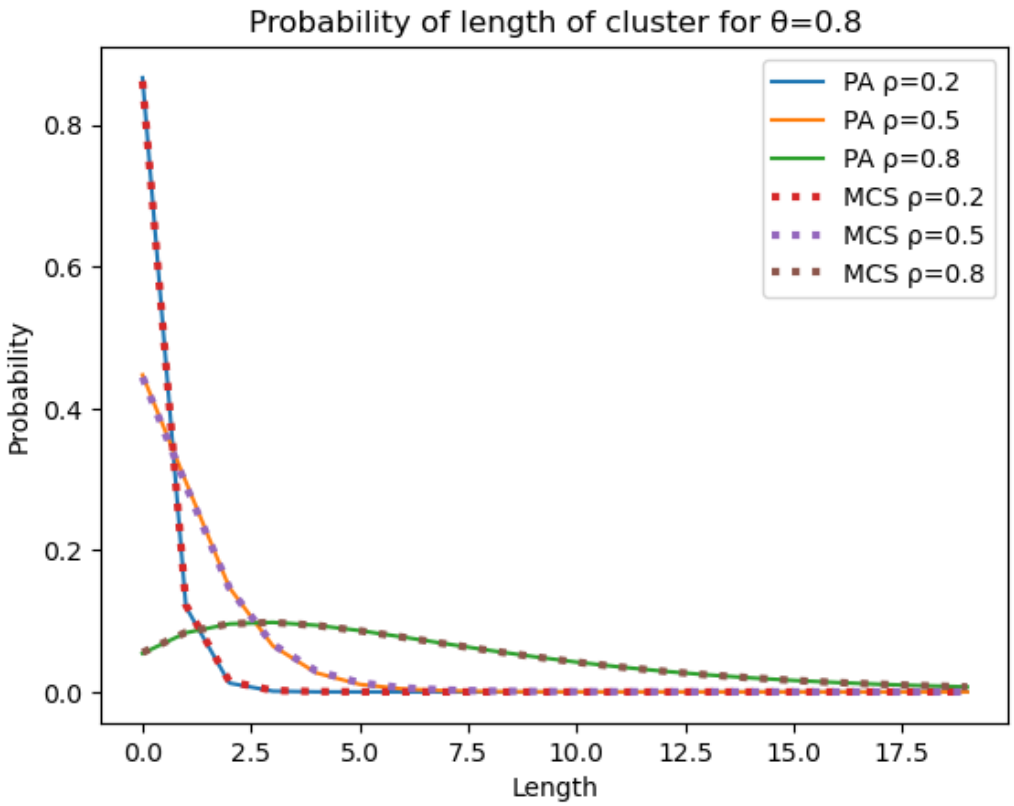

Figure 3: Probability of length of cluster for repulsive regime, $\theta = 0.8$.In solid line we have the results obtained with the theory, while in dot line we have the results obtained by numerical simulations

5.1.2 Critical density of the system for the two different regimes

Here, we are going to confirm that a critical density exists and affects the behavior of our probability and we try to find an analytic theory to determine its value. To find it, we study different values of the density and the interaction parameter θ, and we find the critical density as the density for which $p(1) = p(2)$, this means that the probability of having a cluster of length 1, i.e. a single particle, is equal to have a cluster of length 2, both for numerical simulations and for theoretical part. Using eq. (5.1.2), we find that the condition became:

$$(1-z)^2(1-2z) = 0 \tag{5.1.3}$$

This equation is solved for $z = 1$ and $z = \frac{1}{2}$, that using eq. (5.1.1) correspond to:

$$\phi = \rho \ \wedge \ \phi = \frac{\rho}{2} \tag{5.1.4}$$

The first equality is not interesting because this condition happens only for $\rho = 0 \vee \rho = 1$ where we can not have a dynamics of the model because we have respectively all the site not occupied or all occupied. The second condition is interesting and using the eq. (3.0.19), we can find the expression of the curve in fig. 4. In fig. 4, we can see that numerical simulations and analytical theory perfectly agree in the prediction of the critical density. Note that below the curve we have a monotonic behavior of the probability distribution function, whereas above the curve we have a non-monotonic behavior.

After this we focus our attention to understand the transient behavior of our model.

5.2 Transient behavior

To study the transient behavior of our model, we consider a initial condition with two bulks with a selected density, introducing two shocks. We take the length of this two bulk asymmetric, so we cannot have possible symmetries. In our case we take the first bulk $\frac{3}{5}$ of the system long, and the other ones, obviously, $\frac{2}{5}$ of the system long. So, we have to impose two initial different density in order to obtain the two shocks. To do this, for every interval, we introduce an amount of particle, that can be done simply setting at 1 our occupation state variable σ_i, where i is randomly chosen from the set of indices in the interval consider, such that we obtain the initial density. For all

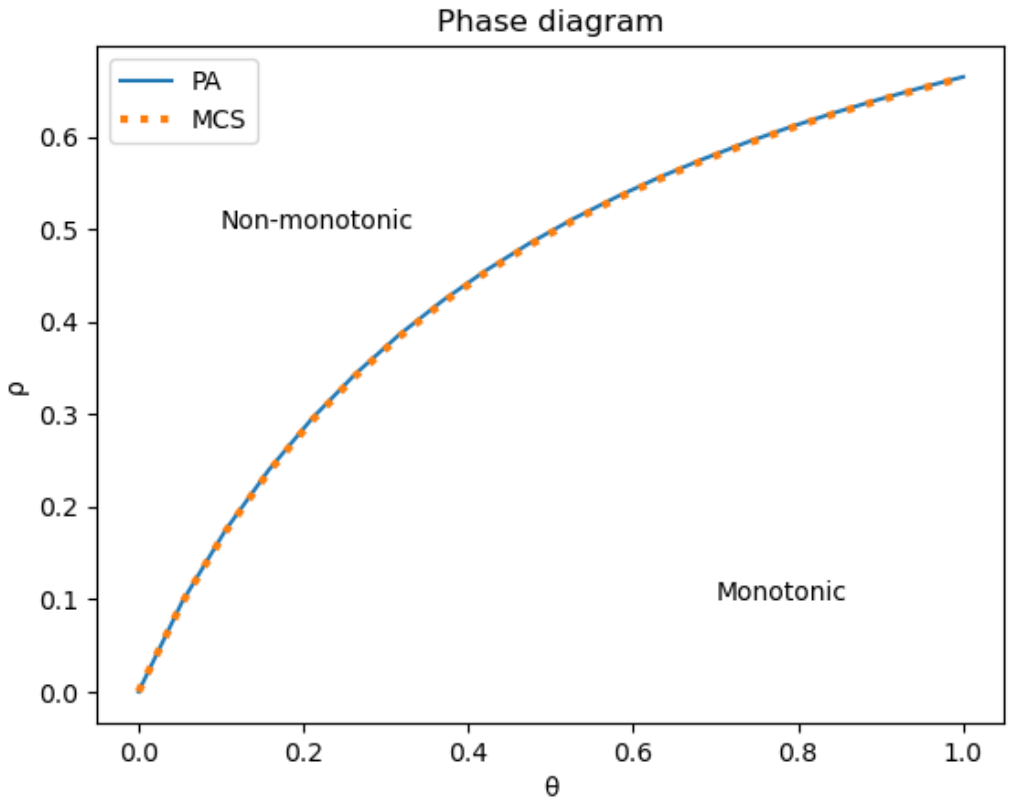

Figure 4: Phase diagram. We represents the critical density in the plane $\theta - \rho$. Above it we have a non-monotonic behavior and below it we have a monotonic one. The solid line represent the result obtain with the PA theory, while the dot line represent the result with the numerical simulations.

the configurations chosen, we study the case when $\theta = 0.2$, attractive regime, when $\theta = 0.5$, we recover **TASEP**, and when $\theta = 0.8$, repulsive regime.

In order to numerically integrate the PA dynamical equations, we use the Euler method to evolve in time both the density and the correlation of the model with step size δ, and we use eq. (3.0.10) and eq. (3.0.13) to calculate the time derivative of ρ_i^t and ϕ_i^t respectively. We have found that a suitable size for the Euler step to obtain the full dynamic of our model is $\delta = 0.1$.

After this we try to develop the behavior of our model in a numerical way.

First of all, the evolution of our model is carried out using the Gillespie algorithm, describe in section 4.1, such that it models the hopping of our particle as describe by the TASEP. To do this, we perform N simulation, here $N = 10500$, of the evolution of our model, every time with a different initial configuration of our state variable $\vec{\sigma}$, but always in a way where we recreate the two shocks and the two density of our interval, and at every time step related to the time step δ, use in the Euler method, we check our quantity that we are studying. Once obtaining this N different realization, we mediate all of it to obtain a general behavior of the system.

In the next chapter, we start with two chosen initial condition and we start to analyze the behavior of the density's profile.

5.2.1 Density evolution

The first case we study is a system which is initialized with a density $\rho_{larger} = 0.8$ in the larger bulk, and a density $\rho_{smaller} = 0.4$ in the smallest one.

So, the mean density of our system is $\rho = 0.64$ and this is the value that the local density ρ_i tend to at the steady state, for every site of the system.
First of all, from fig. 5, and the two subsequent figure, we can see that we have different behaviors of approaching the steady state, depending on the interaction parameter θ and the density ρ. In the fig. 5, i.e. in the attractive regime, we can observe that the two shocks moves slowly and the density profile changes very slowly from one time to the others compared to fig. 7, i.e. the repulsive case, in which our density profile tend very fast to the steady state, i.e. tend to uniform the local density to its mean value ρ for every point of the system. In fig. 8, fig. 9 and fig. 10, we report the total density's evolution for two specific point, both of them in the two bulks of the initial configuration, one in the largest and the other in the smallest.

As we can see before, the attractive case needs more times to reach the

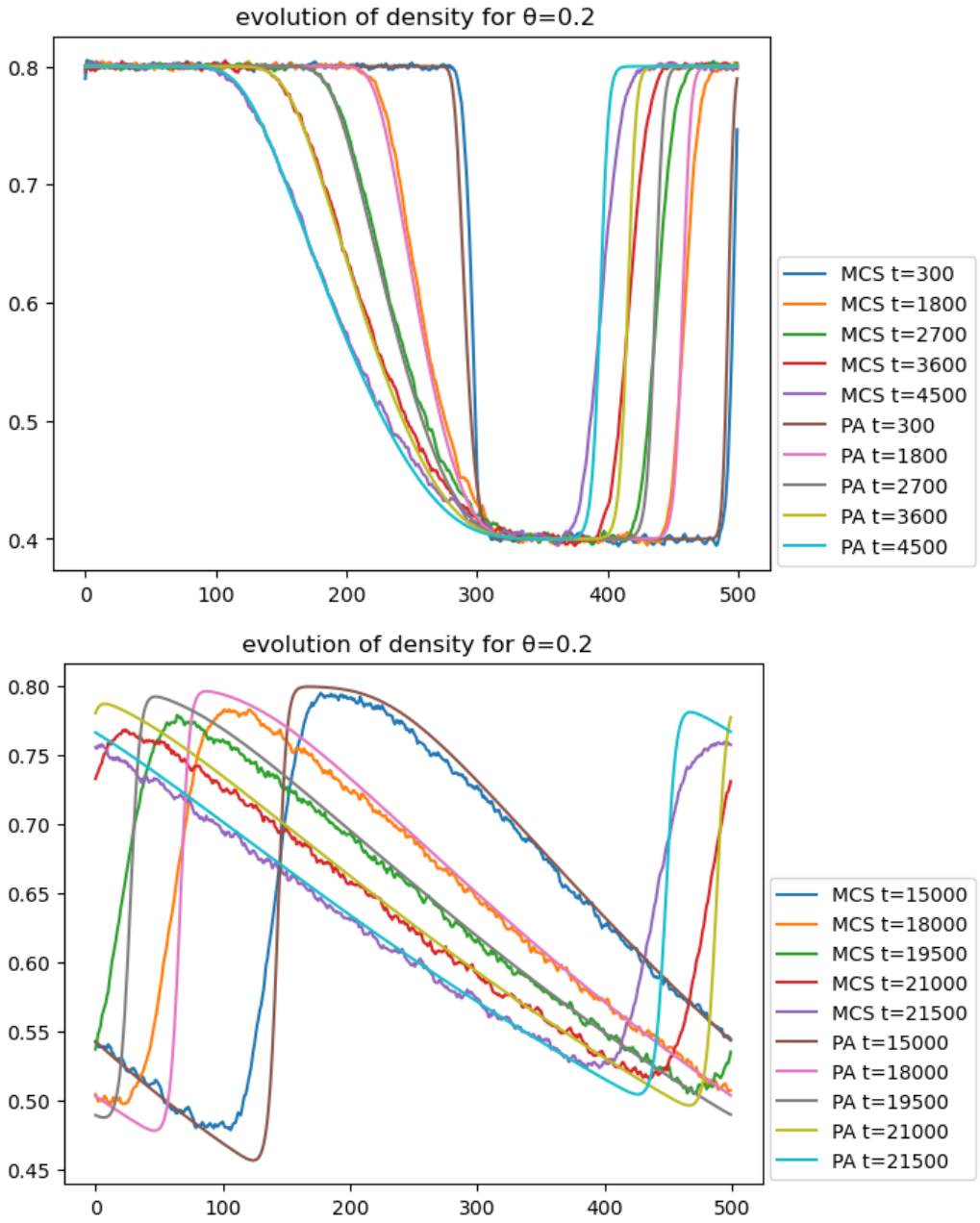

Figure 5: Time evolution of density profile for attractive regime. We present both analytical and numerical results for different time. The smooth lines are the results of PA theory while the others are for numerical simulations.

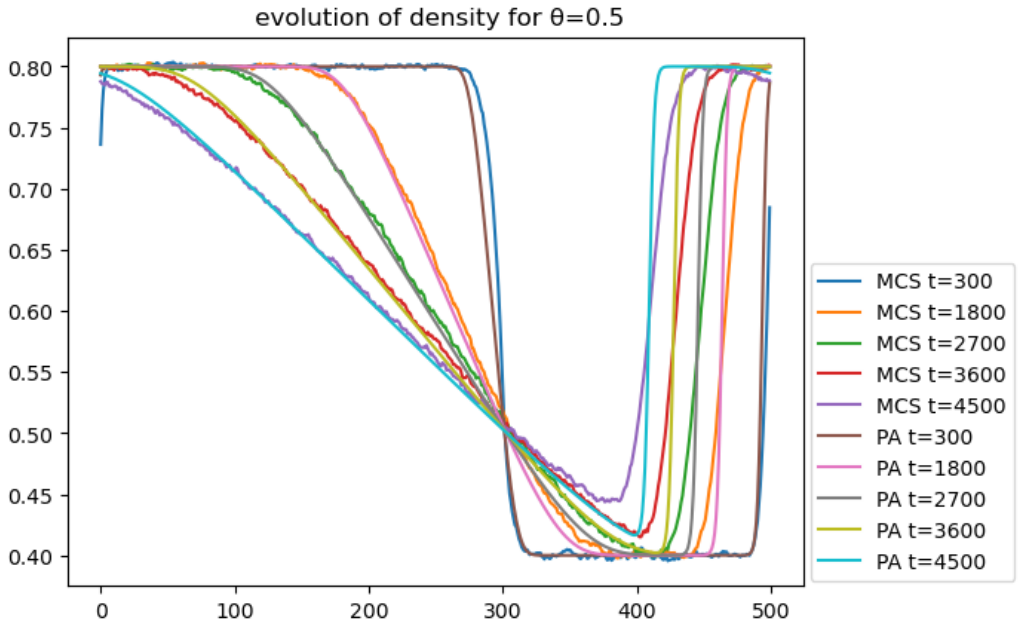

Figure 6: Same of fig. 5, but for pure TASEP.

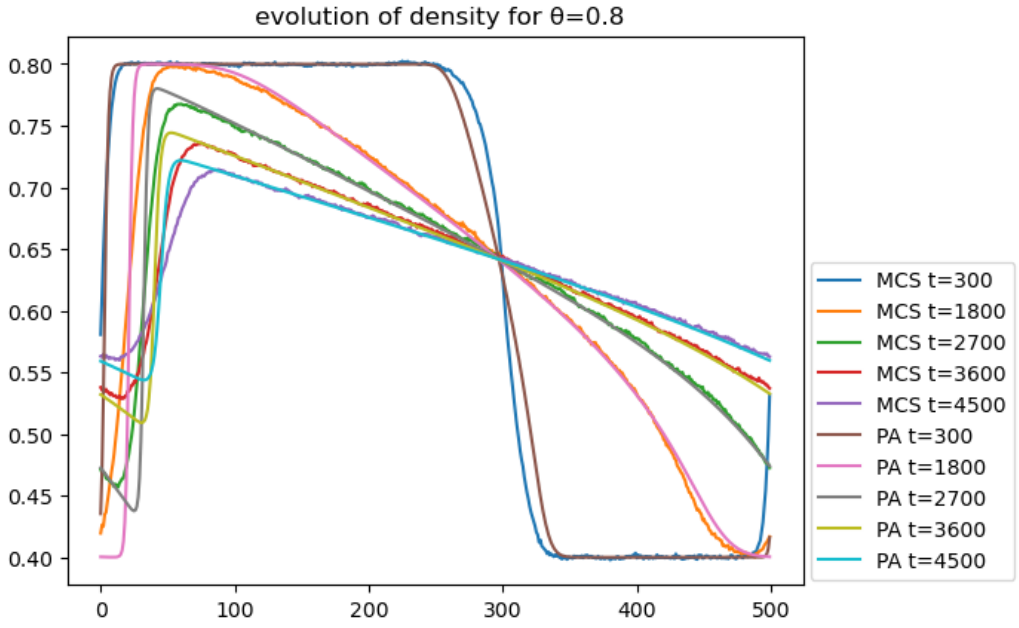

Figure 7: Same of fig. 5, but for repulsive regime

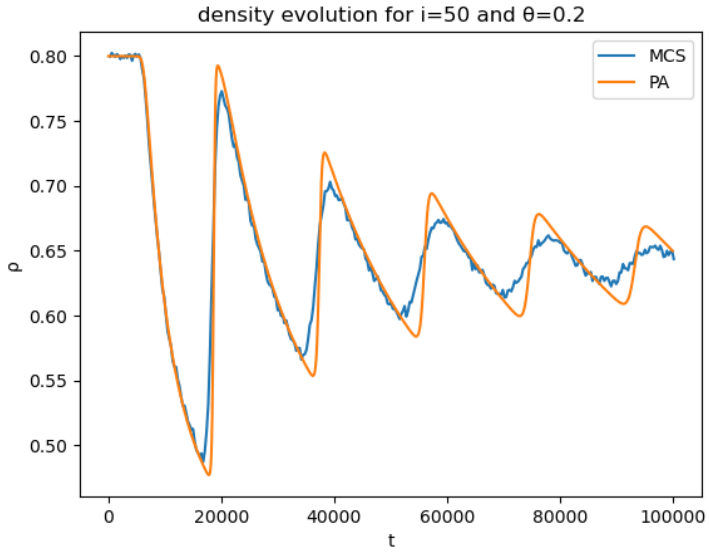

(a) Pos 50, inside the largest bulk.

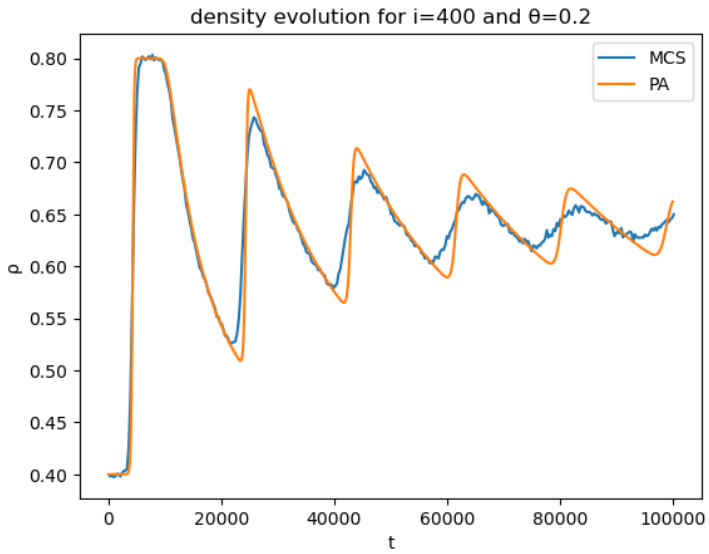

(b) Pos 400, inside the smallest bulk.

Figure 8: Density evolution of two selected point in the attractive regime.

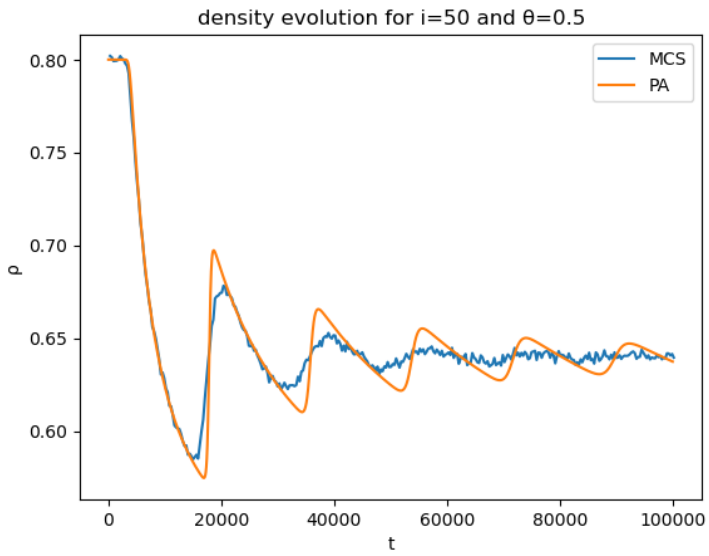

(a) Pos 50, inside largest bulk.

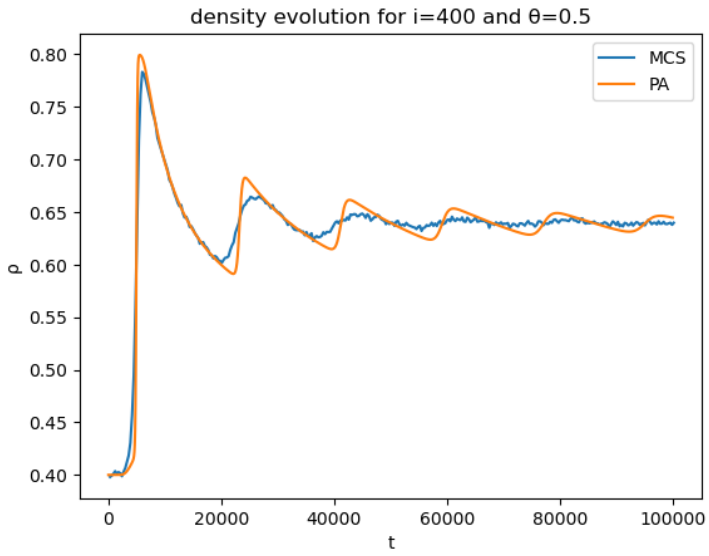

(b) Pos 400, inside smallest bulk.

Figure 9: Density evolution of two selected point in the attractive regime.

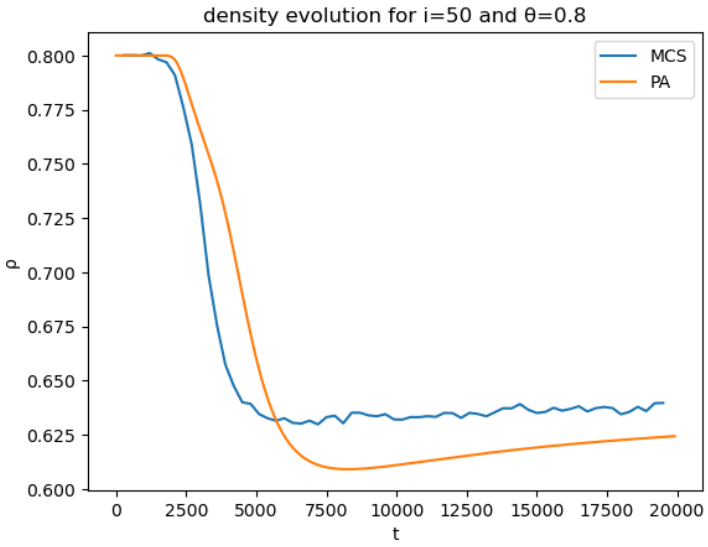

(a) Pos 50, inside largest bulk.

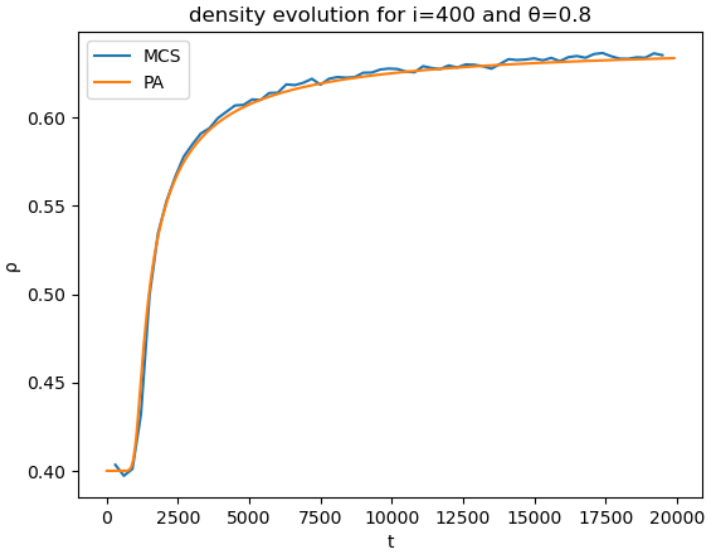

(b) Pos 400, inside smallest bulk

Figure 10: Density evolution of two selected point in the repulsive regime.

steady state, and this can also be understood because we have many oscillations between the maximal and the minimal density, as it can be observed in fig. 8a and in fig. 8b, from this figure we can also observe that the behavior of the model is approximately equal in all the three selected point because our shocks travel around the system many times before its eventually decay.

We can also observe that the behavior of these oscillations is not symmetric. In the descending part we have a smooth inclination that is given by the motion of our diffusing shock that changes smoothly our density, when, conversely, arrives the sharp shock our density goes rapidly to the maximal value of the model and the the inclination of the ascending part is very sharp.

From the same figure, we can see the simulations tend faster to the steady state with respect to the theory's prediction.

Also in fig. 9 we have oscillations, but less frequently than in the fig. 8, that means that it reach the steady state faster, also here the behavior in the two selected point can be consider approximately equal.

In fig. 10, we observe that the system reaches very fast the steady state, without any oscillation. In fig. 10a, we see that the analytical integration of the evolution equation fail to predicts the trajectory, because for the numerical simulations, after a time that remain to ρ_{larger}, it tends rapidly to the mean density ρ, while for the theory, first tend a lower value and after tend to the mean density. While, in fig. 10b, the simulations mimic correctly the behavior of the density, predicts by PA theory.

Also, in fig. 5 and the two subsequent figure, we see that the two shocks present in the initial density moves with some velocity that can have any magnitude and versus, as in fig. 7 the shocks move toward right, while in fig. 5 or fig. 6 they move toward left. Also, one of them diffuses while the other remains sharp, i.e. in fig. 6 the left shock, the one in position 300, diffuses while the right on, in position 500, remains sharp although the maximal and the minimal density change. This behavior is related to the stability of the shock that we can see in section 5.2.5.

Another thing we can observe, in fig. 5-2 and in fig. 7, is that the two shocks at certain time meet themselves and only after this the maximal density start to reduce and tend to the mean one.

The difference in the behavior of our density profile in different regime and the different time need to reach the steady state is related to the position of our mean density with respect to the density of maximal current, as we can see in section 5.2.3. We observe that the farther we are to this quantity, the longest is the time that we need to reach the steady state and so our

system, due to the fact that the two shocks travel among the site, oscillates from the maximal and the minimal value of the model.

The values of the velocity of the shocks are related to θ, this because in general the velocity of a shock, as describe by the Rankine-Hugoniot condition, is defined as the difference between the currents at thee two extremes of the shocks ad the difference of the respective density, as we can see in section 5.2.4, and the current is related to θ through the rate,as describe by eq. (5.2.2).

After this we study one other case in which the stationary density is different, and we see that the velocity of the shock and the time of reach the steady state change. This should be related to the maximal current of the system that we see in section 5.2.3.

As second case, we take again a initial condition with two bulks the same dimension as before, but now the smallest one has a higher density. Therefore we impose that $\rho_{larger} = 0.45$ and $\rho_{smaller} = 0.9$, obtaining a mean density $\rho = 0.63$, that is approximately the same as before and at the steady state the two systems as to tend to the same behavior, as we can observe in fig. 11, fig. 12 and in fig. 13.

Due to the fact that the behavior of the density evolution is similar in both case, for the next subsection we concentrate only in the first case, while this second case are important to understand the symmetry with the Antal-Schutz model. So, we concentrate our study on the behavior of the correlation for the first case.

5.2.2 Correlation evolution

We are also interested in analyzing the behavior of the connected correlation, that is the correlation in which we removes all the possible independent or indirectly fluctuations, define as:

$$\phi_i^c = \phi_i - \rho_i \rho_{i+1} \tag{5.2.1}$$

By this analysis, we can understand how our variable are connected together and how this influences the dynamics. In fig. 14 and the two subsequent figure, the first thing that we note is that the behavior of the dynamical evolution equation for the connected correlation does not mimics the numerical simulations as well as the ones for the density profiles. The second important thing is that we can see that the absolute value of the connected correlation

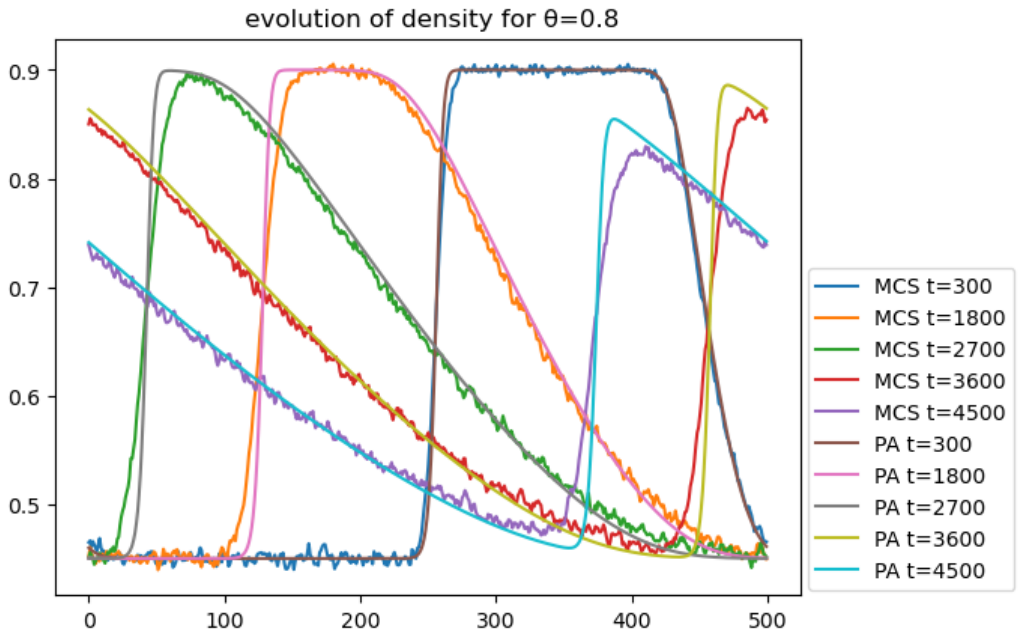

Figure 11: Time evolution of density profile for attractive regime. We present both analytical and numerical results for different time. The smooth lines are the results of PA theory while the others are for numerical simulations.

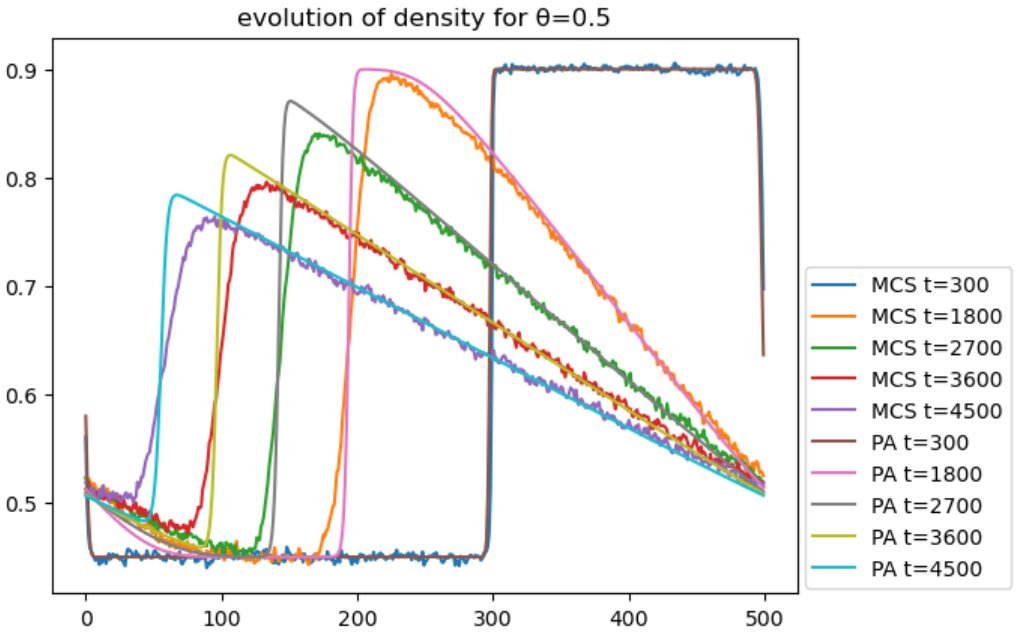

Figure 12: Same of fig. 11, but for pure TASEP.

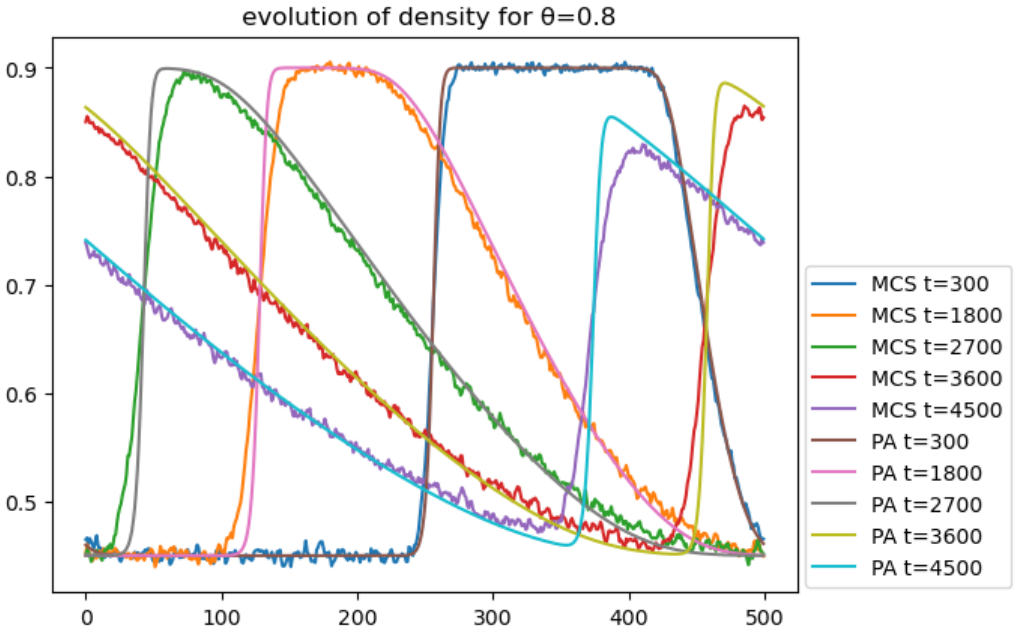

Figure 13: Same of fig. 11, but for repulsive regime

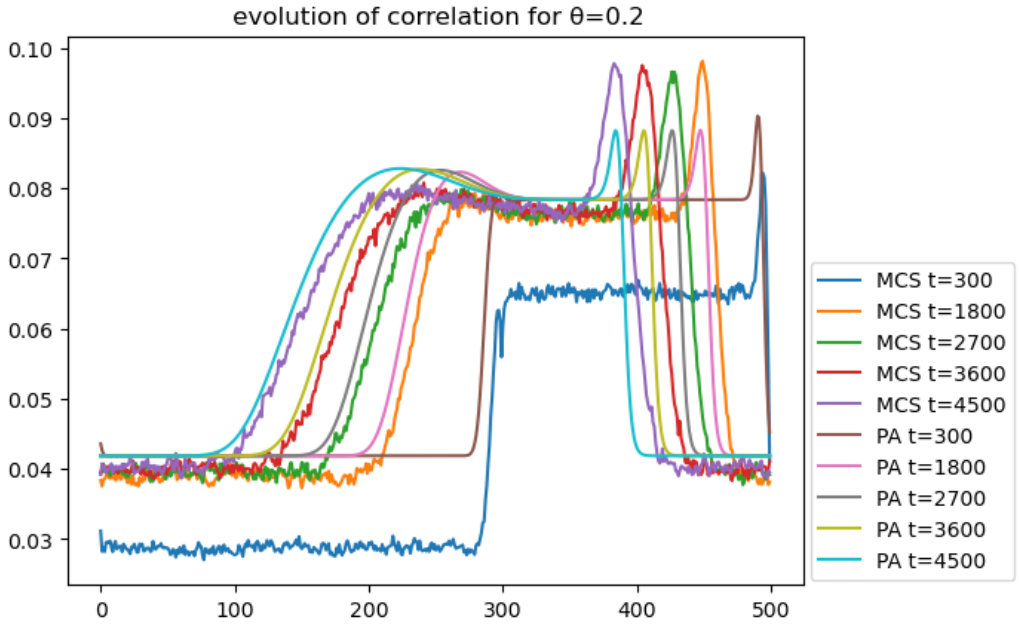

Figure 14: Evolution of the connected correlation for different time in the attractive regime.

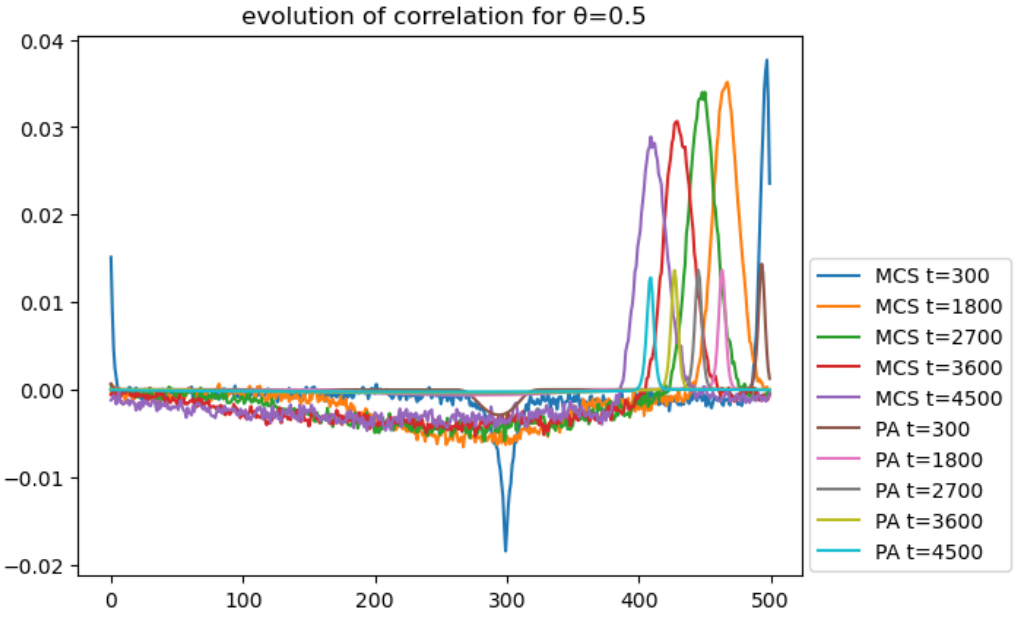

Figure 15: Same as fig. 14, for pure TASEP

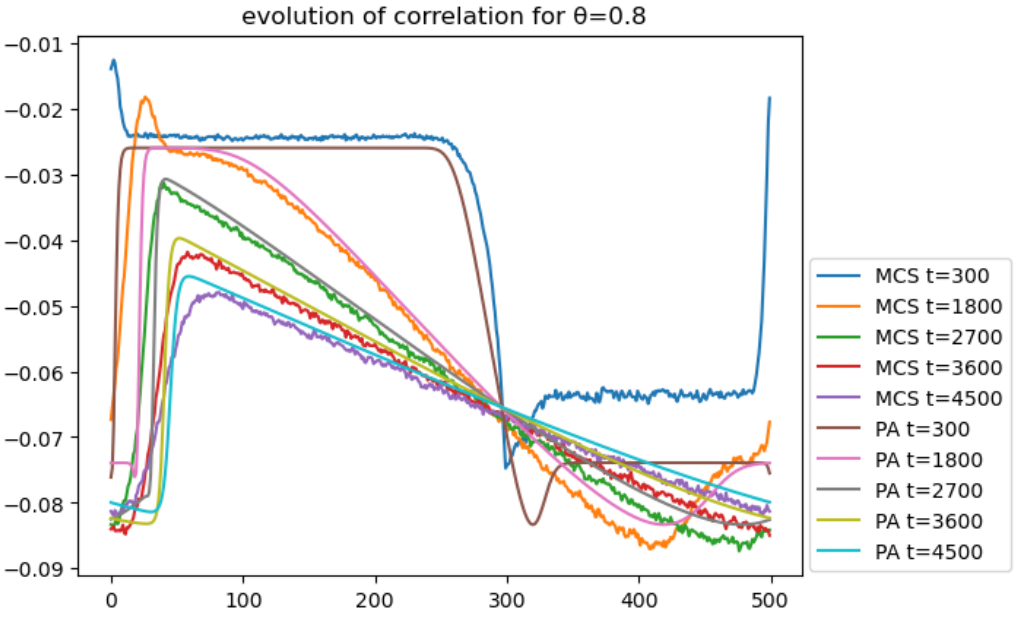

Figure 16: Same as fig. 14, for repulsive regime

are larger in the site in which we have the shocks, meaning that in these sites our variable are more dependent on the others ones.

Also in fig. 15, we can observe that the behavior of pure TASEP is recover, for which all the system are approximately uncorrelated, i.e. the connected correlation is zero, except in the site in which are present the two shocks: the shock that diffuse have a negative correlation and the sharp shock have positive correlation, but the absolute value of this variation is very small.

Instead, in the two other regime the presence of the interaction's energy influences the connected correlation in all of our model, giving a positive background in the attraction regime, and a negative one in the repulsive regime. As before, the shocks amplifies the connected correlation between the particle.

As we do for density profile, we observe the connected correlation profile for the same three different site as before, we can see that in fig. 18 the connected correlation is approximately always zero and it does not influenced by the rapidly change in the density. While in the 2 other regime, presented in fig. 17 and in fig. 19, the connected correlation follows the behavior of the density and when we have a quickly change in the density, caused by the passage of the sharp shock, also it change quickly. This can be seen in fig. 20, where we report one of this rapidly change of the density on the site 400 on the attractive regime, in which we can see that after some little time the connected correlation adapt quickly to this change.

After study the correlation, we study the current of our system that as we can see in eq. (3.0.11), depends on both the density and the correlation of the model.

5.2.3 Current

As we see before, the current play a strategic role in the determination of the time needs by our model to reach the steady state and so in the behavior of the transient. From the article of [1] ,we can find an expression for the current on the steady state:

$$J = \bar{r}(\eta I - (\eta - 1)(a + b\rho)) \tag{5.2.2}$$

where

$$\bar{r} = r\ \frac{p + s - 2q}{r - q},\ a = \frac{r}{r - q} - \frac{p}{p + s},\ b = \frac{p - s}{p + s - 2q} \tag{5.2.3}$$

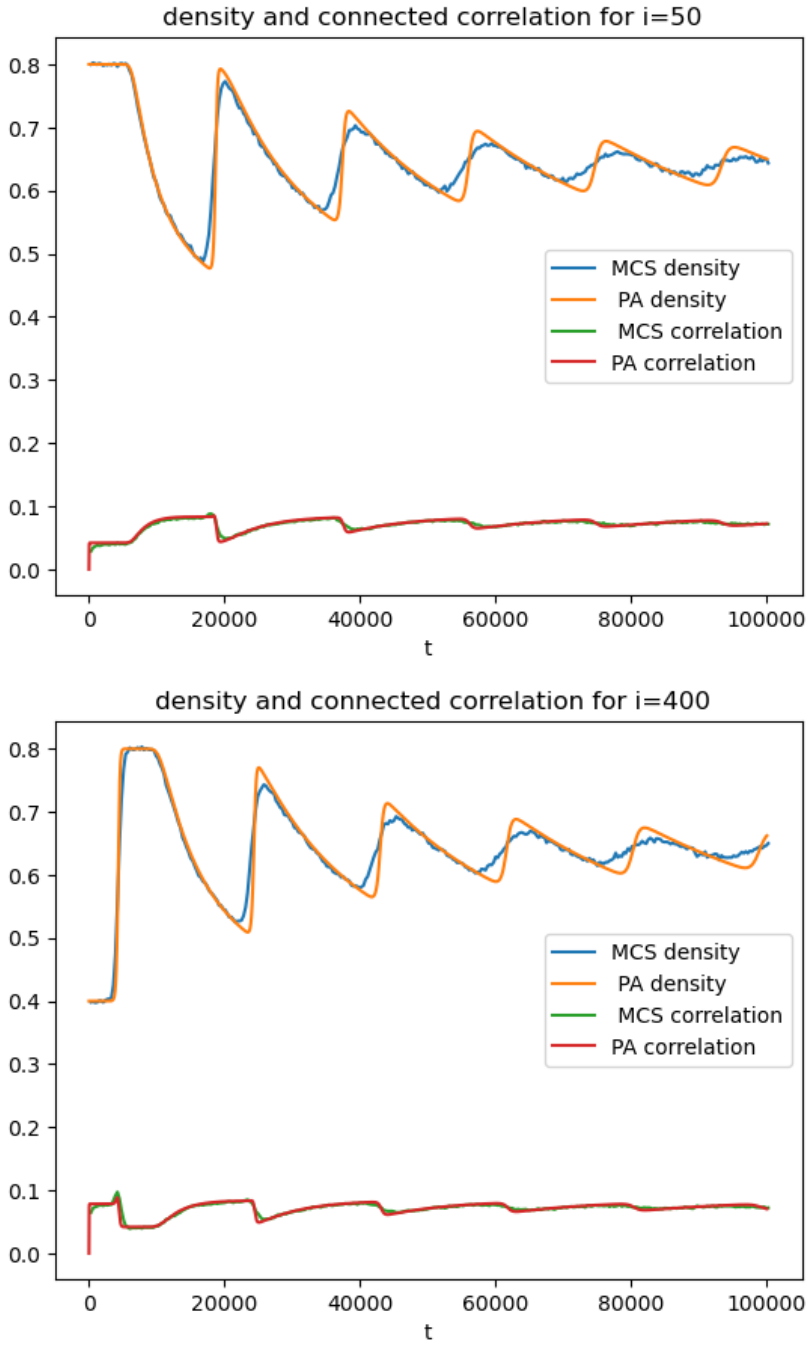

Figure 17: Density and correlation evolution in attractive regime

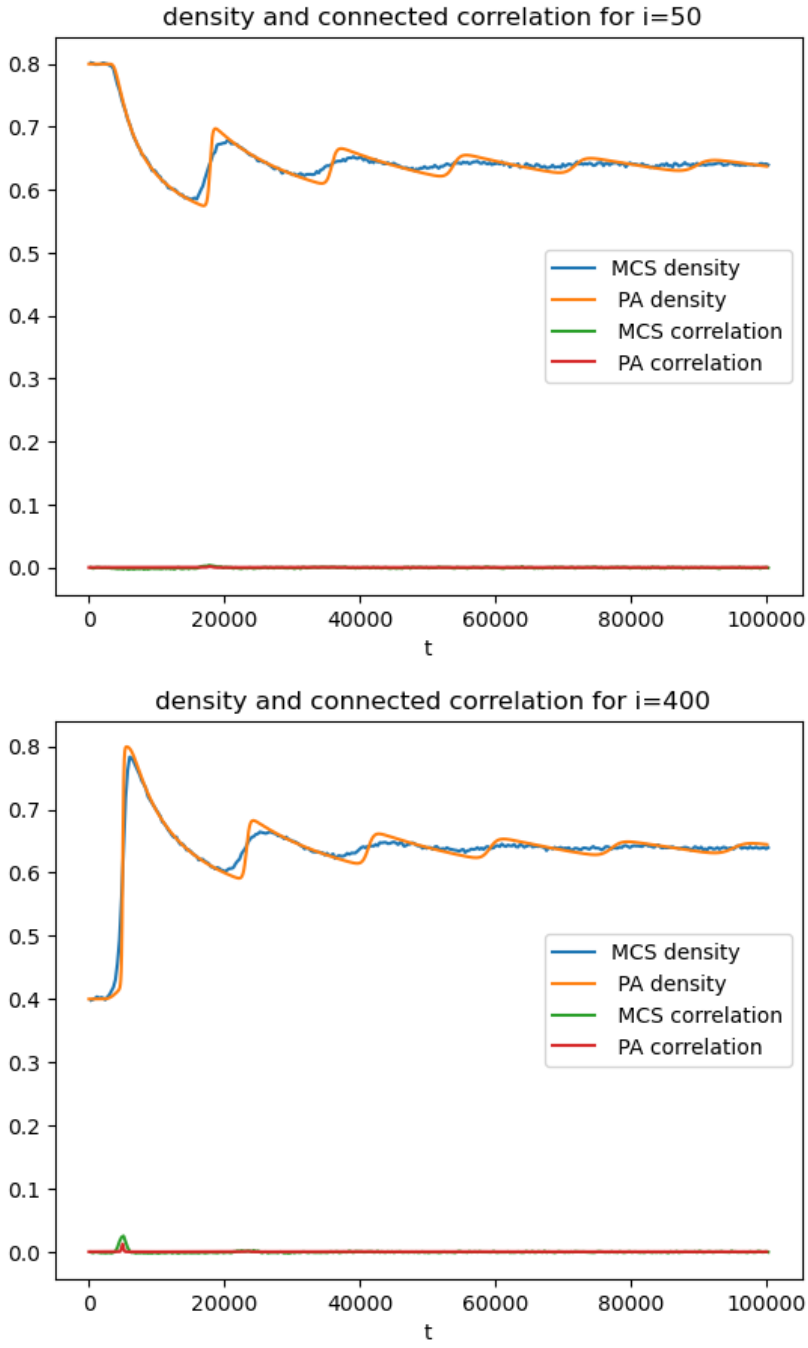

Figure 18: Density and correlation evolution in pure TASEP

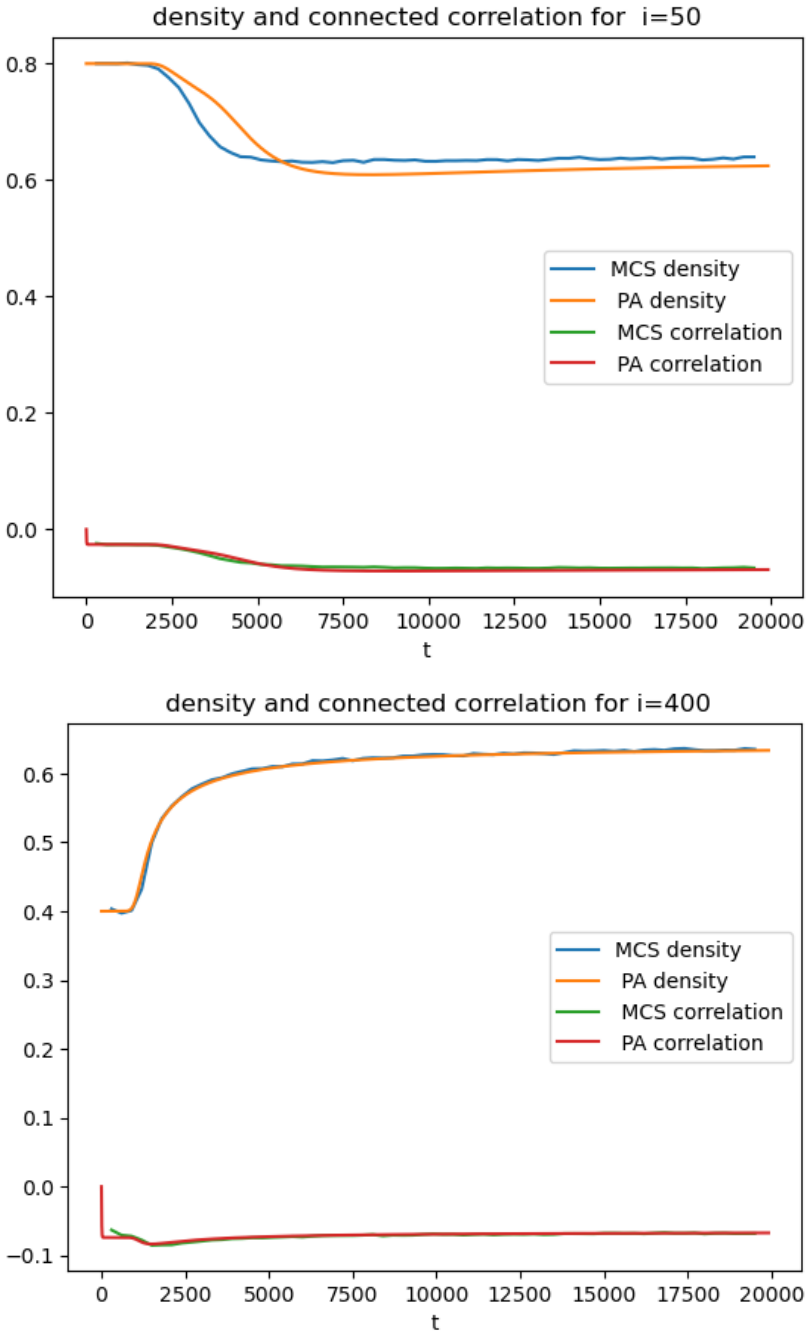

Figure 19: Density and correlation evolution in repulsive regime

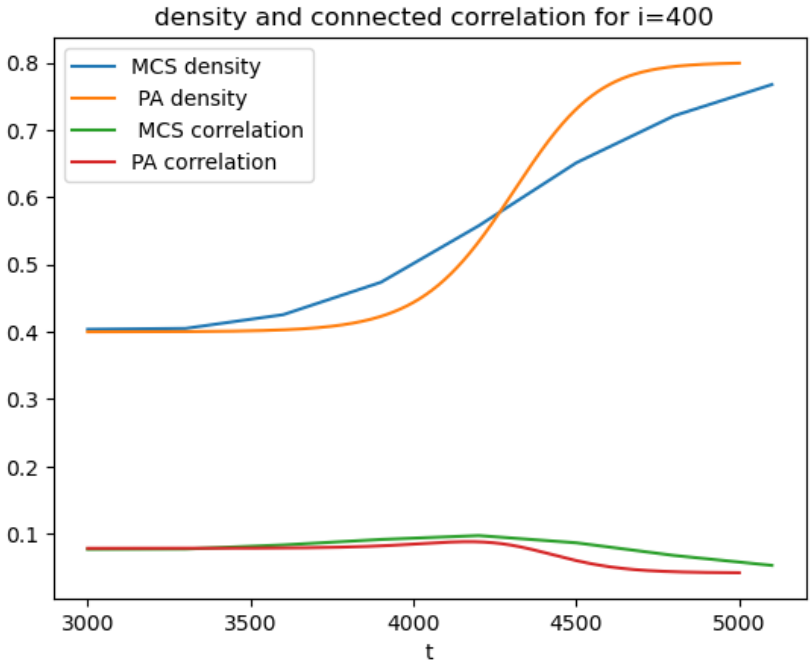

Figure 20: Detail of the evolution of the density and the correlation in site 400 and around time 4000 in the attractive regime.

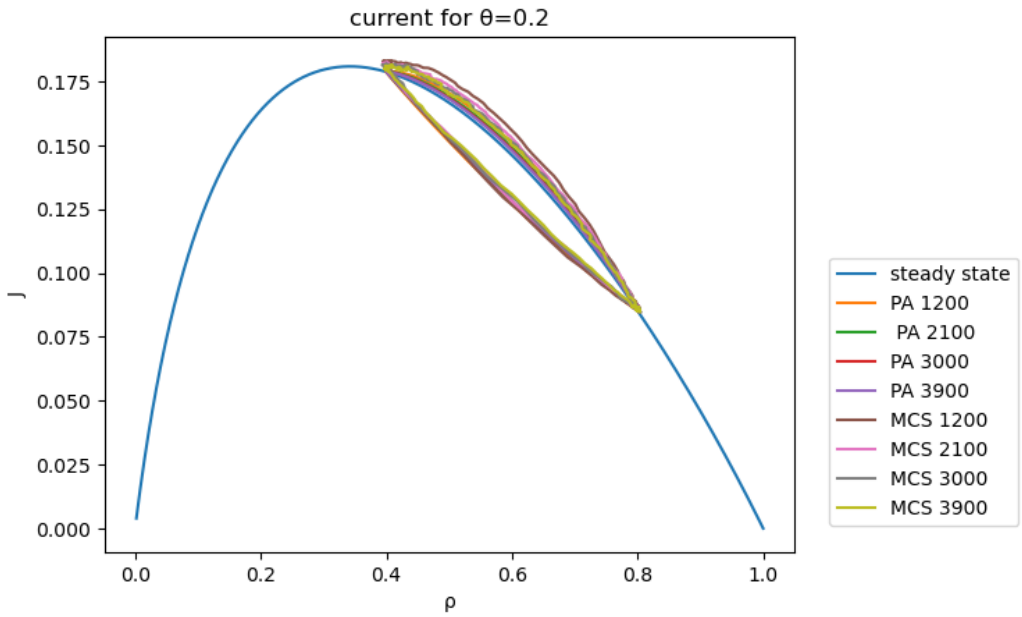

Figure 21: Evolution in time of the system in ρ-J plane in the attractive regime. The blue curve is the current at the steady state, while the smooth close curves are the one given by the integration of the evolution equation at different time and the other close curves are the results of the numerical simulations.

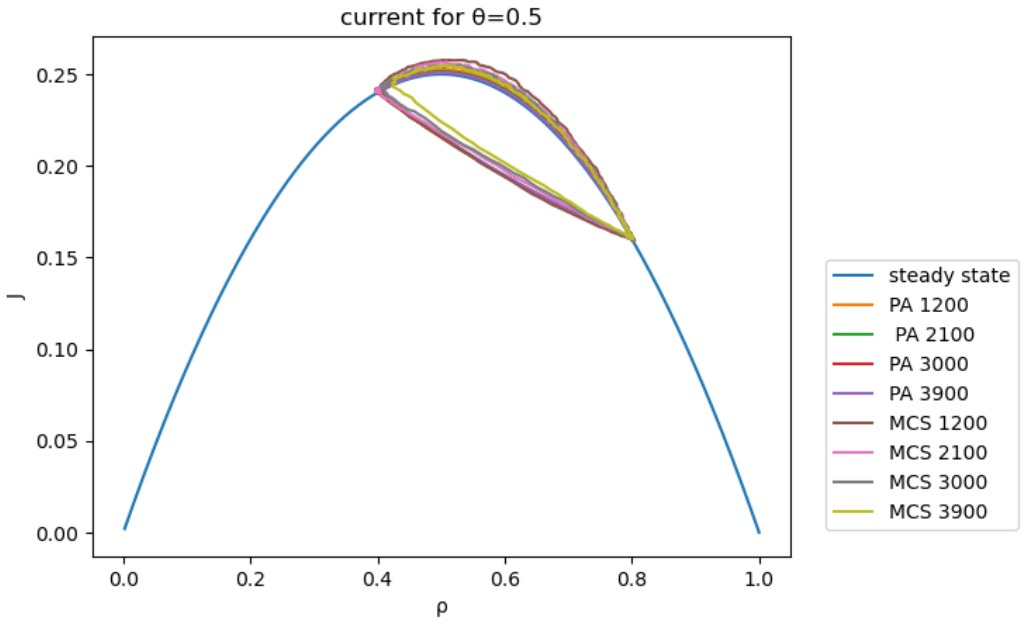

Figure 22: Same as fig. 21, but for the pure TASEP.

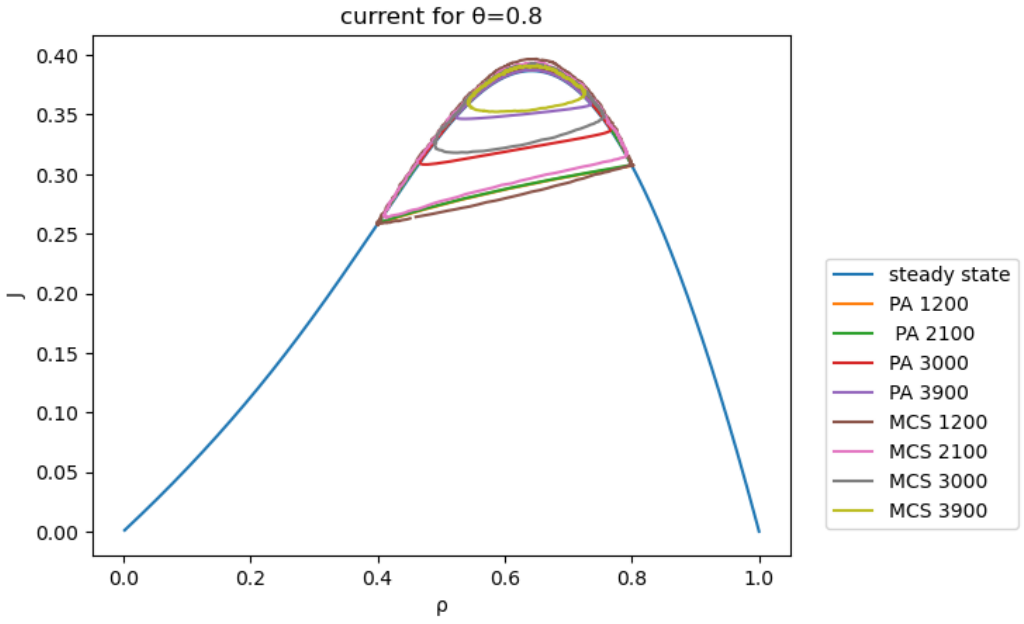

Figure 23: Same as fig. 21, but for the repulsive regime.

In the case of the Facilitated model, we obtain $\bar{r} = e^{\beta E}$, $a = 1.0$ $b = -1.0$.

In fig. 21, fig. 22 and fig. 23, the blue curve is the value of the current in the steady state given by eq. (5.2.2), and the close curves are the evolution of both the theoretical model, in which we use the values of ρ_i^t and ϕ_i^t, obtained with the integration of the evolution equations, in eq. (3.0.11) to find the value of the current of our model, and we plot the value of J for the different values of ρ in our model, and for the numerical simulations. Also here we have good agreement between the two part, as expected.

We observe that through the flow of time this close curve tend to the values of the current of the steady state.

In fig. 24, we can understand clearly the behavior of the close curve in fig. 21 and the subsequent 2 figures.

First of all we can see in fig. 24b that the site in the two bulks of our configuration have all the same current that coincides to the values calculated in steady state with eq. (5.2.2).

After this we noticed that we have the sharp shock in position 1 and the diffusive one in position 300. The sharp shock induces a rapidly change in the current of our model from position 1 to position 2, this implies in fig. 24a the straight line from the point A and we reach the point ρ-J predicts by the theory, going on our density-current profile we remain in the same point until we are in the bulk and when we reach the diffusive shock, it tries to mimic the curve at the steady state until we reach the other bulk density and we again obtain correctly obtained the values at the steady state and remain again here until we reach the other site of the stable shock, that again change quickly the value of the current and because this in fig. 24a we have the straight curve.

So, we see that the diffusive shocks tends to mimic the value of the current at the steady state and going through the time it fits more and more the curve at the steady state until it reach it, when we obtain the steady state that become approximately a point because we have the same density in every point and so the same current.

Also we can see in the next chapter how the current influences the behavior of the velocity of the shock.

5.2.4 Velocity of shock

We have seen that the shocks in the density profile move in different ways as in fig. 5 we have a negative velocity, while in fig. 7 we have a positive

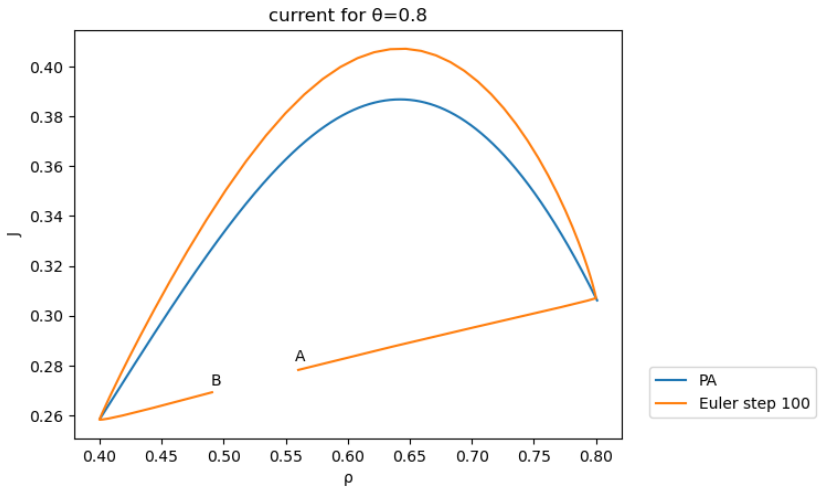

(a) ρ-J plane. We can see the current at the steady state obtained by eq. (5.2.2), blue curve, and the curve obtained after integrating the evolution equation after 100 Euler step,orange curve. The point A correspond to the site 1 in the adjacent figure and the point B to the site 500

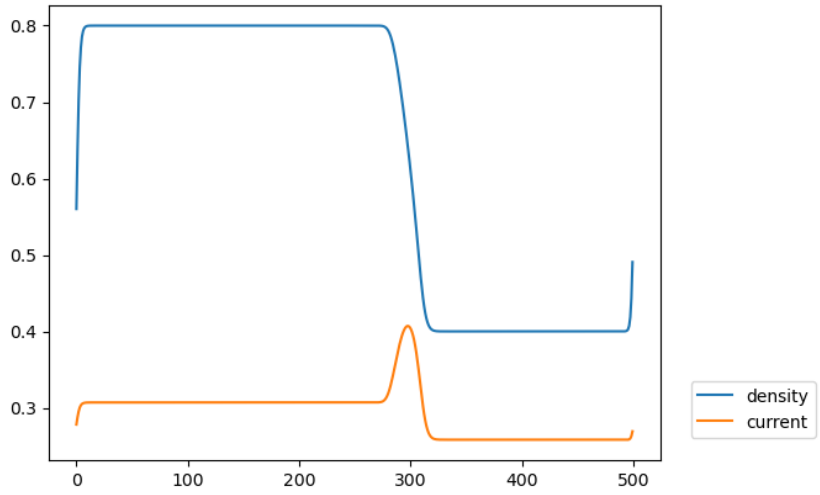

(b) Current and density after 100 Euler step.

Figure 24: Detail of the current of the system after 100 Euler step with $\rho = 0.64$ and $\theta = 0.8$

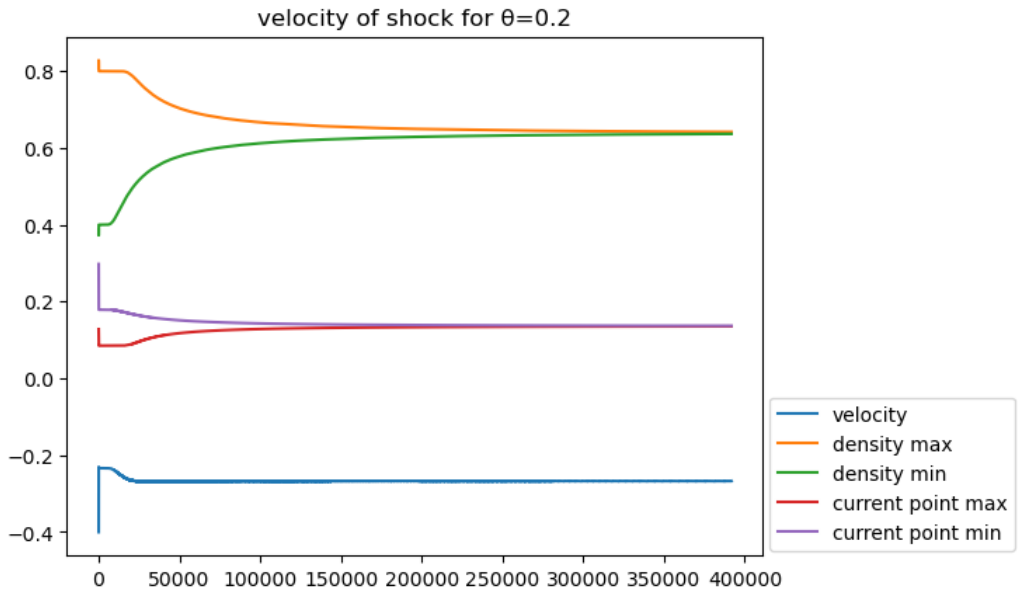

Figure 25: Velocity of shocks for the attractive regime. As shown in legend the blue curve is the velocity of the shock while the orange and the green lines are respectively the maximal and minimal density of our system, that are at the two extremes of the shock, and the red and purple lines are respectively the current of the maximal density point and the minimal one.

one, so we are interested in calculating the velocity of the propagation of our shocks. To calculate the velocity predicted by the theory, we use the *Rankine-Hugoniot* jump condition:

$$v_s = \frac{J(\rho_R) - J(\rho_L)}{\rho_R - \rho_L} \tag{5.2.4}$$

where indices R(right) and L(left) refer to the position with respect to the shock.

As we have seen in the time evolution of the density profile, in fig. 25, fig. 26 and fig. 27, we can have positive or negative velocity, depending on the regime we consider.

This is related to the fact that from eq. (5.2.4), the velocity depends only on the difference of the current and the density at the two sides of the shock, and due to the fact that our model tends to have the same density in all the points, the shock moves towards the mean density of the system of the curve

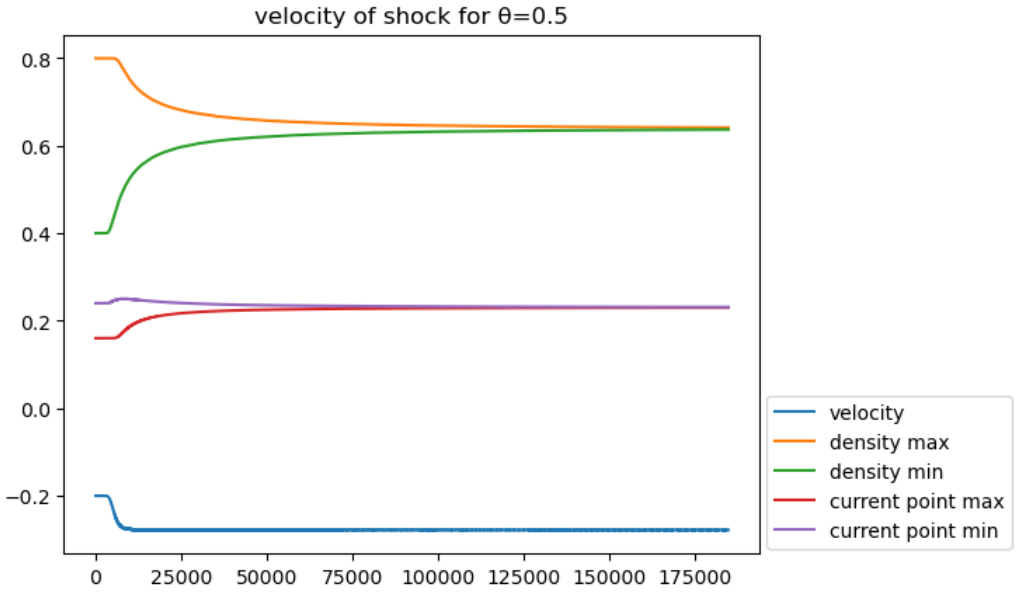

Figure 26: Same as fig. 25, for the pure TASEP

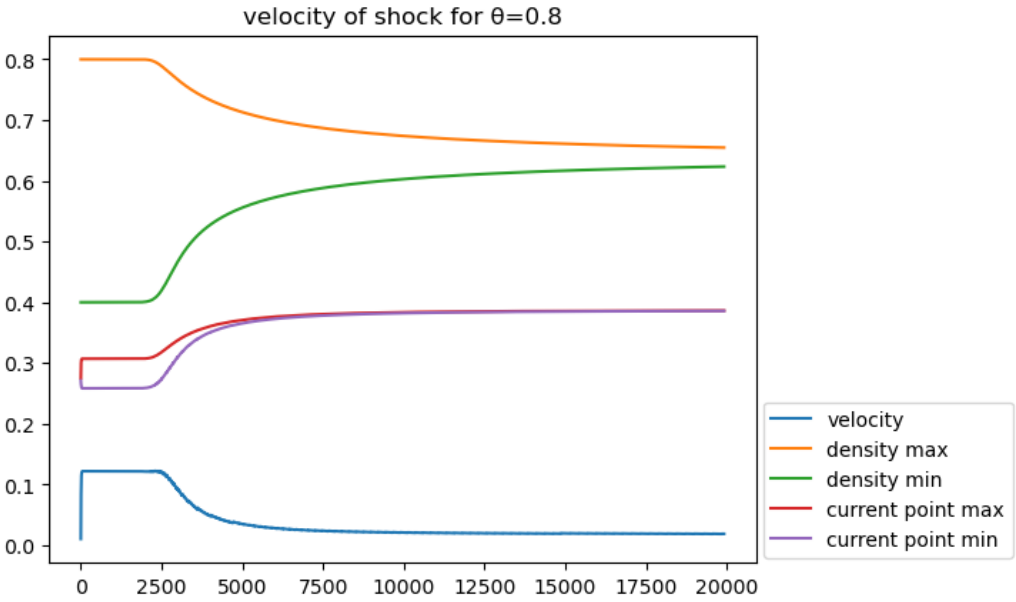

Figure 27: Same as fig. 25, for the repulsive regime

of the steady state in the plane ρ-J.

Also we observe a plateau at the beginning of the evolution, this is related to the fact that, as we can see in the fig. 25,the densities on the two sides of the shock and, therefore, the respective currents do not change. This happens because, as we can see in fig. 5, the density and also the current in the two bulks does not change until the extremes of the shock meet each other, that happens because the spreading of the left shock. Therefore, due the expression of eq. (5.2.4), as long as this quantity remains constant also the velocity is constant.

Then, when the first density starts to change, usually the minimal density, also the velocity change, but as soon as also the second density change, the velocity returns constant,because this density reduction happens at the same velocity in both the maximal point and the minimal one such that eq. (5.2.4) remains constant, until it reaches stationarity.

In fig. 5, we have seen that one of the two shock spreads, while the other remains sharp. The reason of this behavior can be understood in the next subsection.

5.2.5 Stability of shock

In this chapter we want to understand when a shock is stable or unstable.

From [3], we know a stability criterion for a single shock, that is:

$$v_g(\rho_L) > v_s > v_g(\rho_R) \tag{5.2.5}$$

where v_s is the velocity of the shock, calculated with eq. (5.2.4), v_g is the group velocity of the particles calculated as $v_g = \frac{dJ(\rho)}{d\rho}$ and indices R and L, again, label the two extremes of the shocks.

A shock is stable under this condition because at every interaction the excess density will drift back to the shock position and it stabilize it. While, if we do not have this condition, the excess density velocity are in the different direction, i.e. the value is always the same but the position of the two are exchange, leading to a smear out of the shock. In our model we can see it in fig. 28 and fig. 29, where due to the fact we have the same density and current at the extreme of the shocks and so the have the same group velocity in this point. So, the only things that decides which shock is stable is eq. (5.2.5), because when we consider the right shock we have $v_g(\rho_L) > v_g(\rho_R)$ so it is stable in this case, while on the left shock left and right are exchange and so

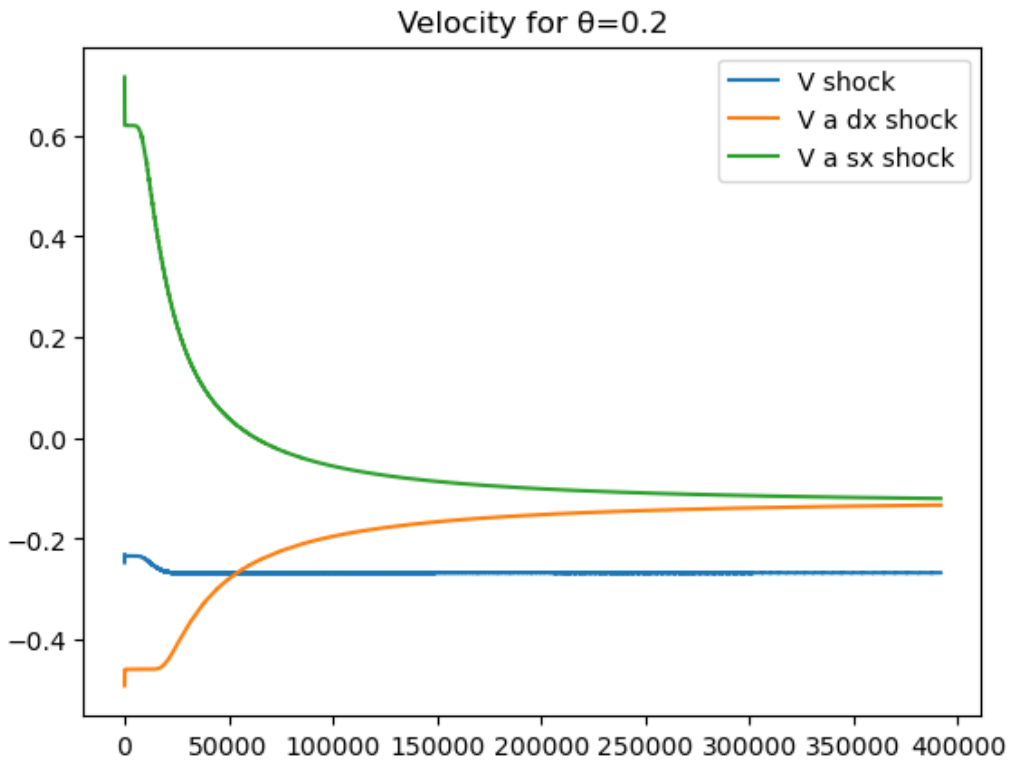

Figure 28: Stability of the right shock in the repulsive regime, $\theta = 0.2$. The Blue curve is the velocity of the shock, while the green curve is the group velocity on the left side of the shocks and the orange curve is the group velocity on the right.

the previous expression are no longer valid and because of this the shock is unstable.

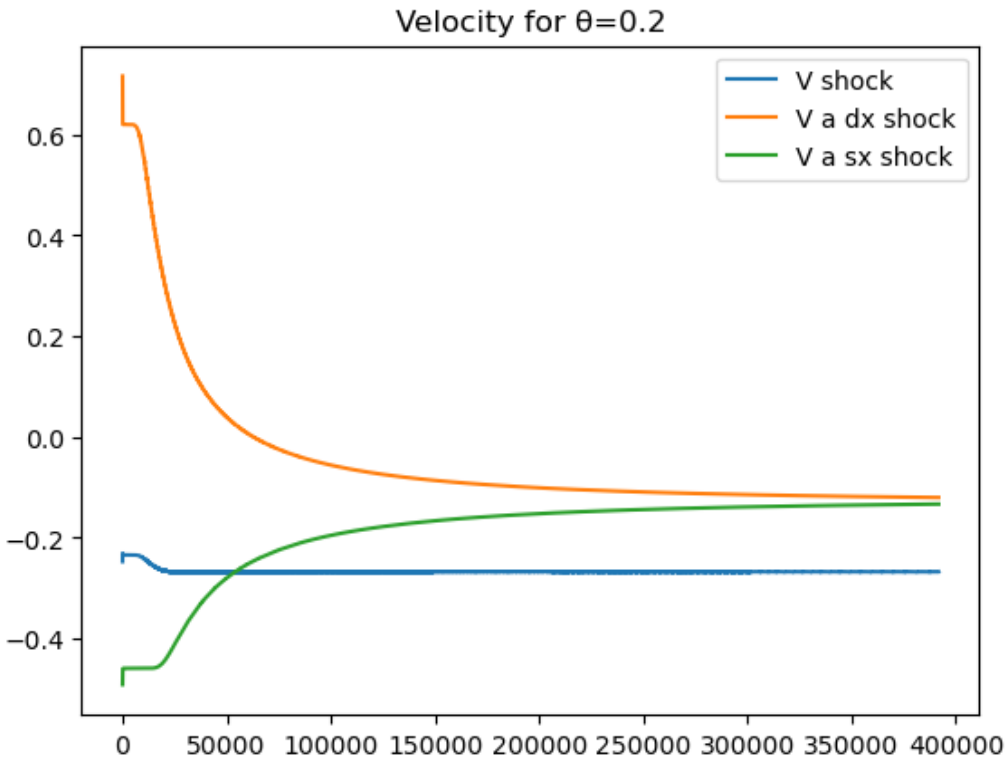

Figure 29: Same as fig. 28 but for the left shock.

6 Antal-Schütz model

In this section, we consider the Antal-Schütz's model and we want to describe the result we obtain and compare them to the results obtained from the Facilitated Model's.

6.1 Steady state

As we do in section 5.1, we initialize our variable state $\vec{\sigma}$ with a defined configuration such that we obtain a precise density. Again we let the system evolve until it reaches stationarity, using the current as check variable, as we do before.

Once we reach the stationarity, we can start to analyze the behavior of the cluster's length, as we do before, to see if there are present some symmetry, as we expected.

6.1.1 Cluster's length

Due to the particle-hole symmetry described in eq. (2.0.11), we are interested to calculate the probability distribution of the cluster's length of the hole, the cluster of hole is a group of consecutive site that are not occupied by the particle. We study it in a numerical way similar to the one used in the Facilitated model, and we find the same behavior of the Facilitated Model but why interaction parameter $1 - \theta$, as we can see in fig. 30. This confirm the existence of the symmetry describe before.

The symmetry with respect to the site position is no longer important at the steady state because it is independent on the position.

Now, we check if the criterion ,find in section 5.1.2, predicts also the value of the critical density for the hole for this model and therefore the symmetry.

6.1.2 Critical density of the system for the two different regimes

Therefore, we calculate the critical density as done before for the Facilitated Model, finding that this symmetry is confirmed, as we can see in fig. 31.

Now, we start to analyze the transient behavior to find proof of this kind of symmetry in the transient behavior.

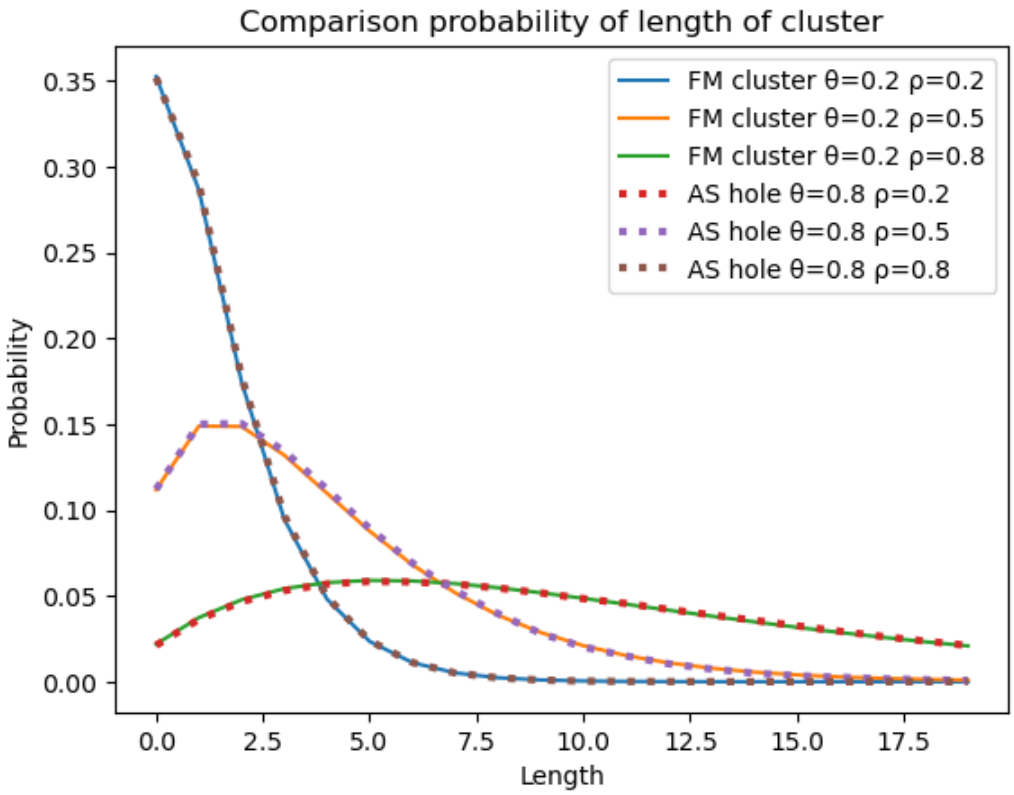

Figure 30: Comparison of the behavior of the length of cluster at three different density of Facilitated Model with $\theta = 0.2$, in solid line, and the length of cluster of hole in Antal-Schütz Model with $\theta = 0.8$, in dot line.

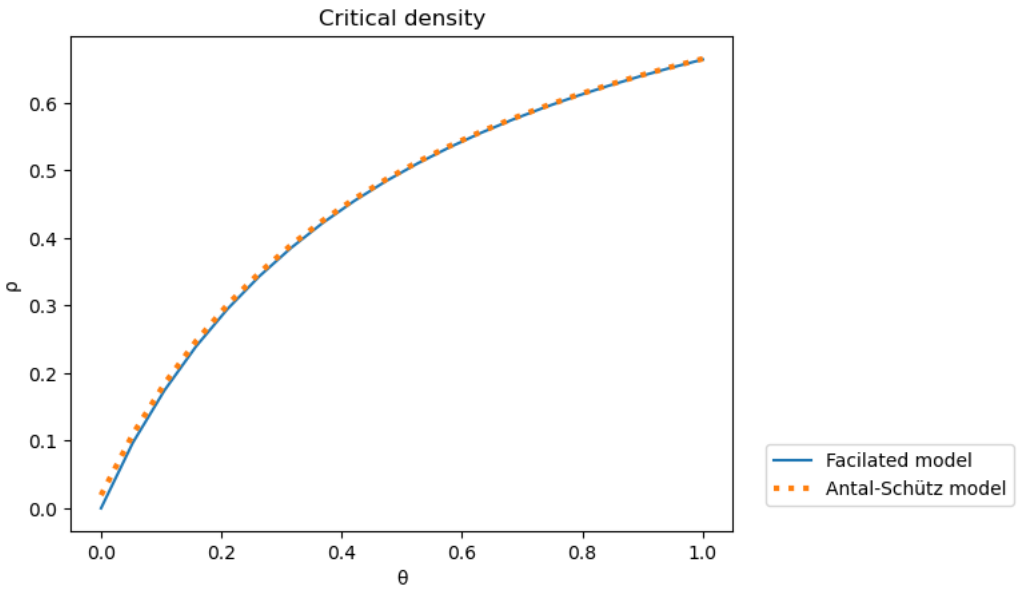

Figure 31: In this graph we compared the critical density obtained in the Facilitated model, solid line, with the critical density obtained in the Antal-Schütz model, dot line, while we use a interaction parameter $1 - \theta$.

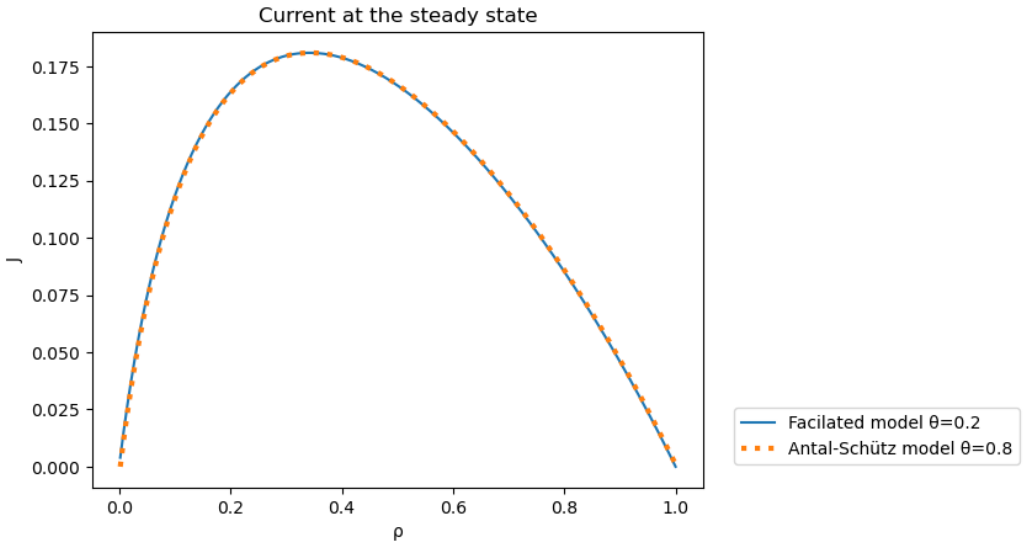

Figure 32: Comparison the current at the steady state for $\theta = 0.2$ in the Facilitated Model, in solid line, and for $\theta = 0.8$ for the Antal-Schütz Model, in dot line.

6.2 Transient behavior

To study the transient phase of our model, we do the same step done for the Facilitated model to develop the various results. As we can see in the next section the results are very similar and again all the dynamics depends only on the density ρ of the system and on the interaction parameter θ.

6.2.1 Current

As we seen before in section 5.2.3, the current is important to determine the behavior of the transient and the time to reach the steady state. From the article of [1] ,we find eq. (5.2.2) that described the current at the steady state. The parameter present in the formula change in the Antal-Schütz model because are related to the rate describe in table 1.Here we obtain $\bar{r} = e^{\beta E}$, $a = 0.0$ $b = 1.0$. Indeed we can observe in fig. 32 that the particle-hole symmetry is present in the current at the steady state. So, this symmetry reflects on all the transient behavior of our model and, obviously if we consider the first case introduce before we are in a total different regions of the plane ρ-J, as we can see in fig. 33 and fig. 35, so the relaxation time and the density evolution

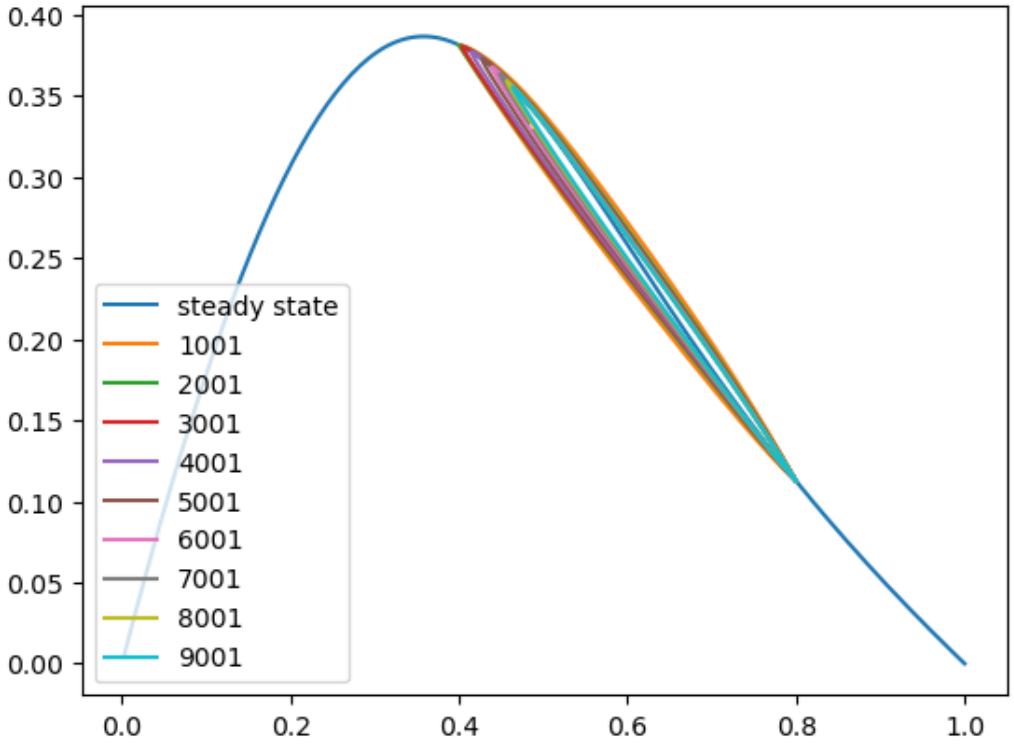

Figure 33: Evolution in time of the system in ρ-J plane in the attractive regime. The blue curve is the current at the steady state, while the other close curve are the one given by the integration of the evolution equation at different time

are totally different as we can see in the next subsections. Obviously the behavior when we have No inteactions, i.e. pure TASEP, doesn't change for the symmetry of the model, as we can see in fig. 34

6.2.2 Density evolution

As we see in the previous subsection, in we consider the first case, we are in a totally different point of the plane ρ-J, so we expect totally different behavior of the transient. This is confirmed observing fig. 36 and in fig. 38, where the behavior is quite different. In fig. 36, we can see that also the sharp shock tends to spreads over the time, related again to its stability. Indeed in fig. 38, we can see that the velocity of the shock is slower with respect the one in fig. 7

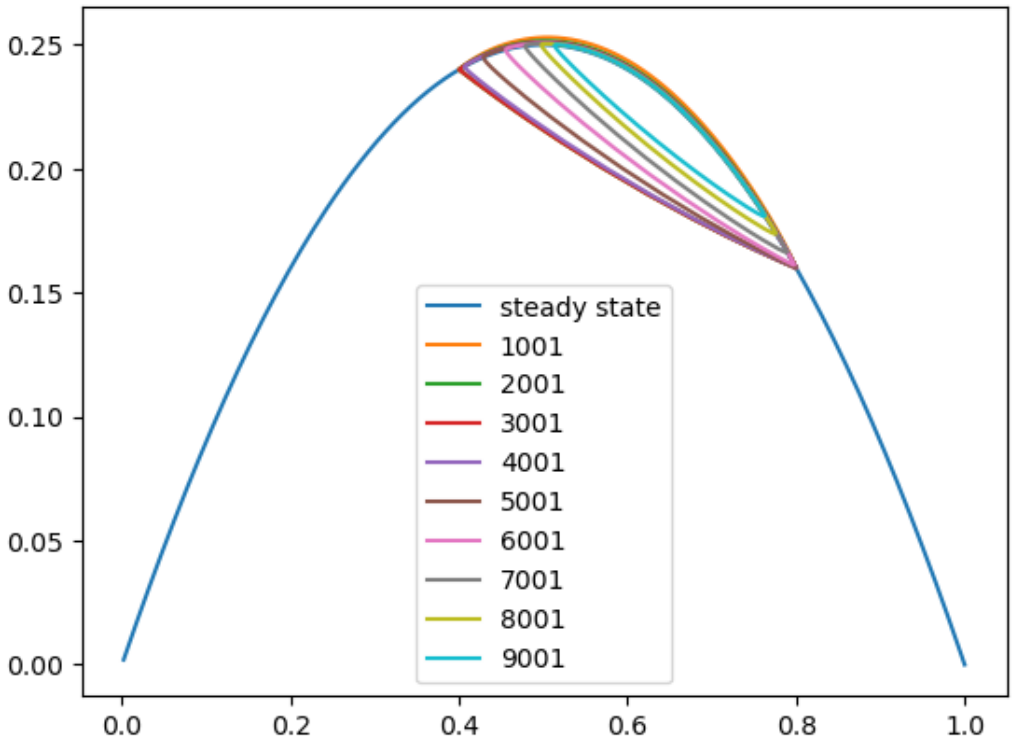

Figure 34: Same as fig. 33, but for the TASEP

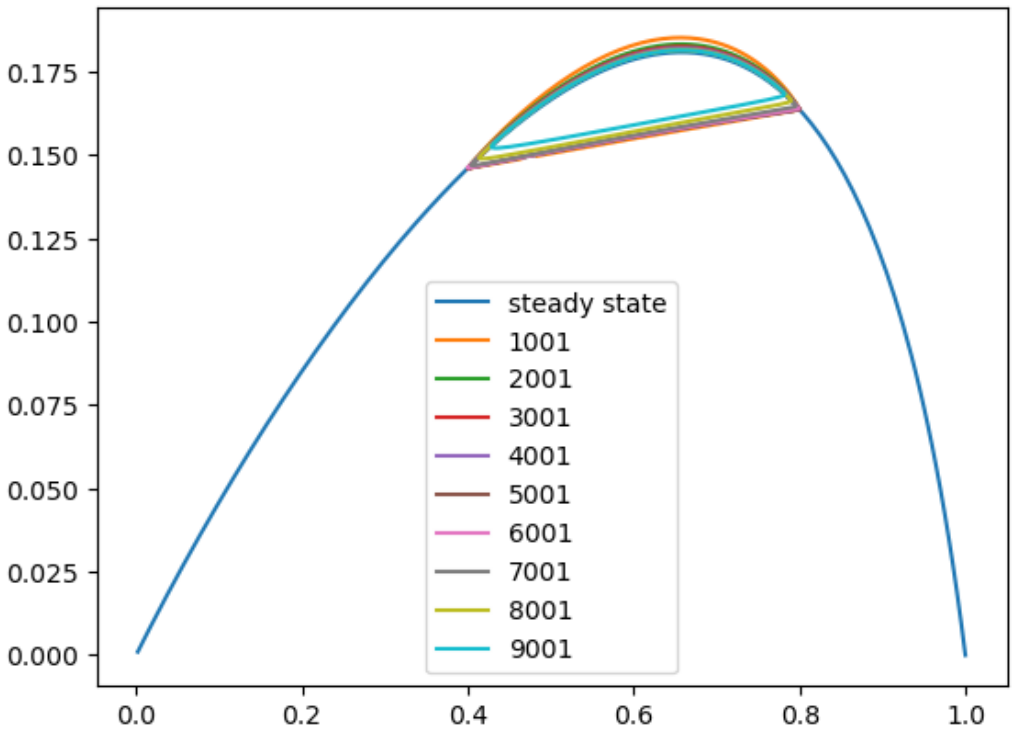

Figure 35: Same as fig. 33, but for the repulsive regime

and also the relaxation time is larger. So, here we have different behavior that as the same properties describe in section 5 and so a quite repetitive analysis. Instead, a interesting case is to try to understand the presence of the symmetry between the two case. For doing so, we takes the second case discussed in the Facilitated Model and try to apply this symmetry. First of all, we have to reverse the initial condition imposed before. Therefore if before we set $\rho_{larger} = 0.45$ and $\rho_{smaller} = 0.9$, now using the symmetry $\rho \Rightarrow 1 - \rho$, we set $\rho_{larger} = 0.55$ and $\rho_{smaller} = 0.1$, such that the mean density is $\rho = 0.37$. Now we let the system evolves as define before and we consider for the Facilitated Model the case with $\theta = 0.8$ represent in fig. 13 and the case for the Antal-Schütz model with $\theta = 0.2$, represent in fig. 39. If we compared the two figures the presence of the symmetry is not clearly distinguishable but, if we revers all the point in the two bulks, i.e. point 1 exchange with point 300 and so on, also for the second bulk, we obtained fig. 40, where we can clearly see that the two behavior coincides.

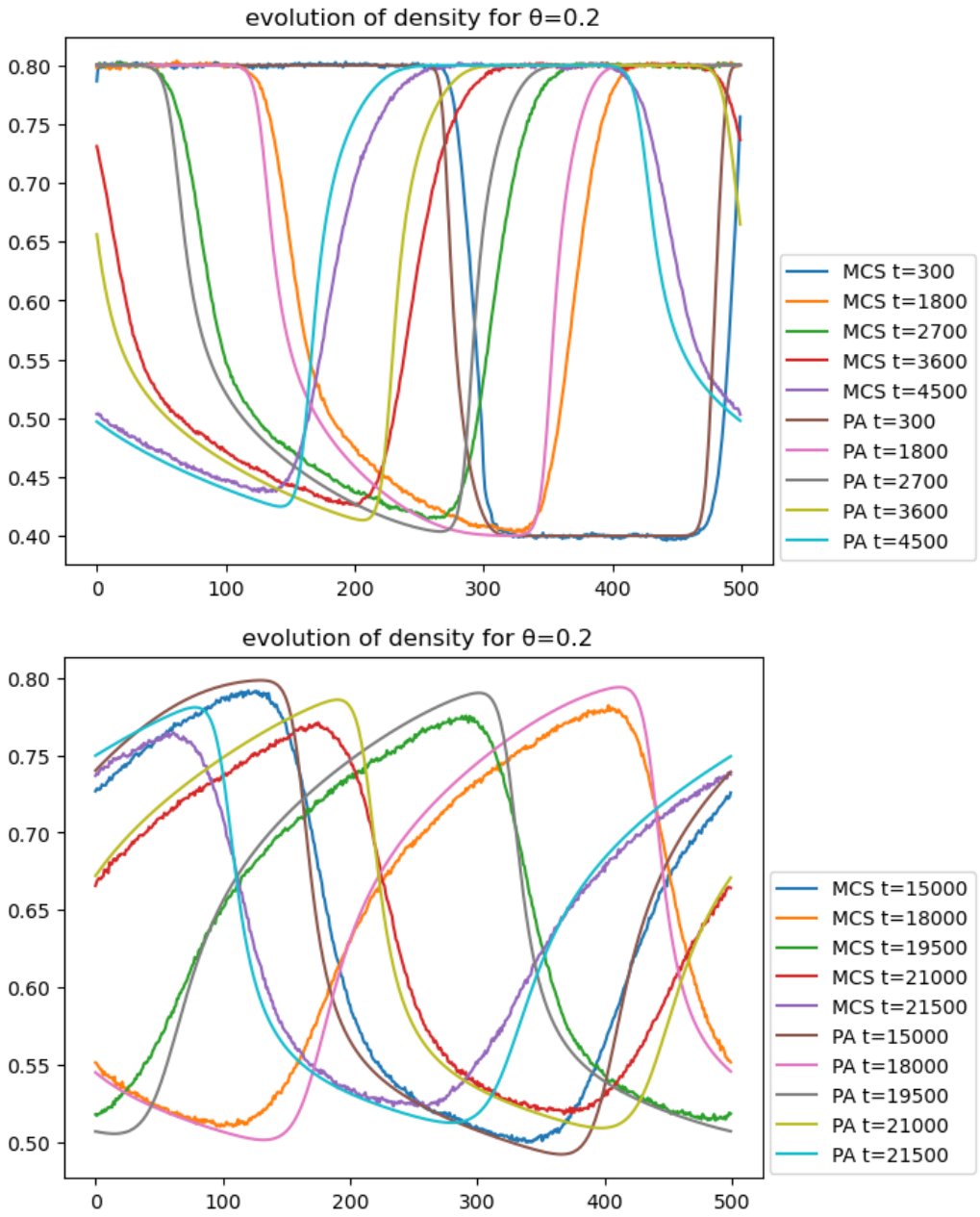

Figure 36: Time evolution of density profile for repulsive regime. We present both analytical and numerical results for different time. The smooth lines are the results of PA theory while the others are for numerical simulations.

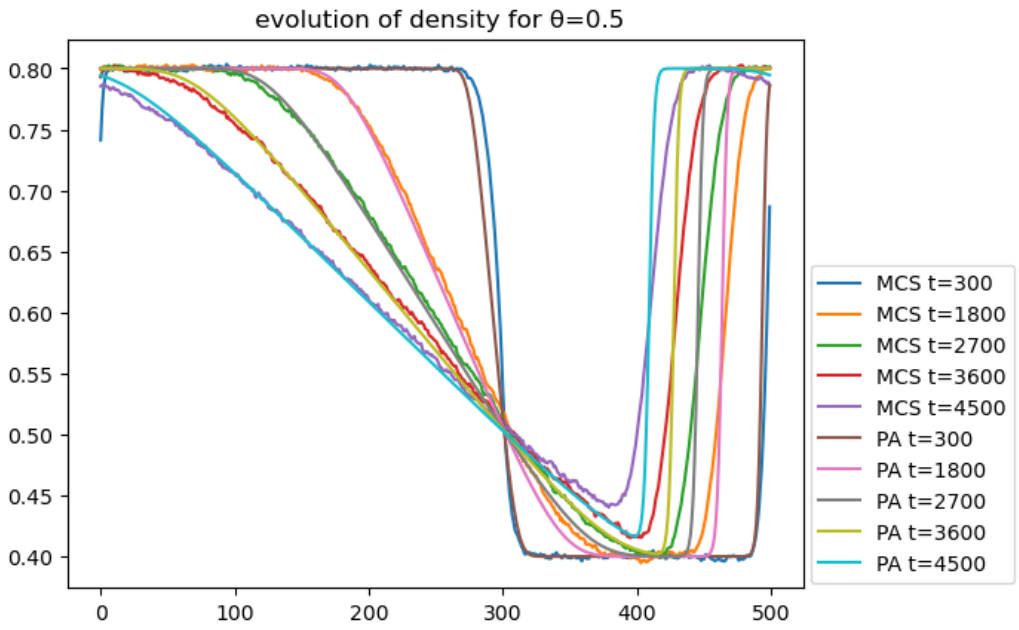

Figure 37: Same of fig. 36, but for pure TASEP.

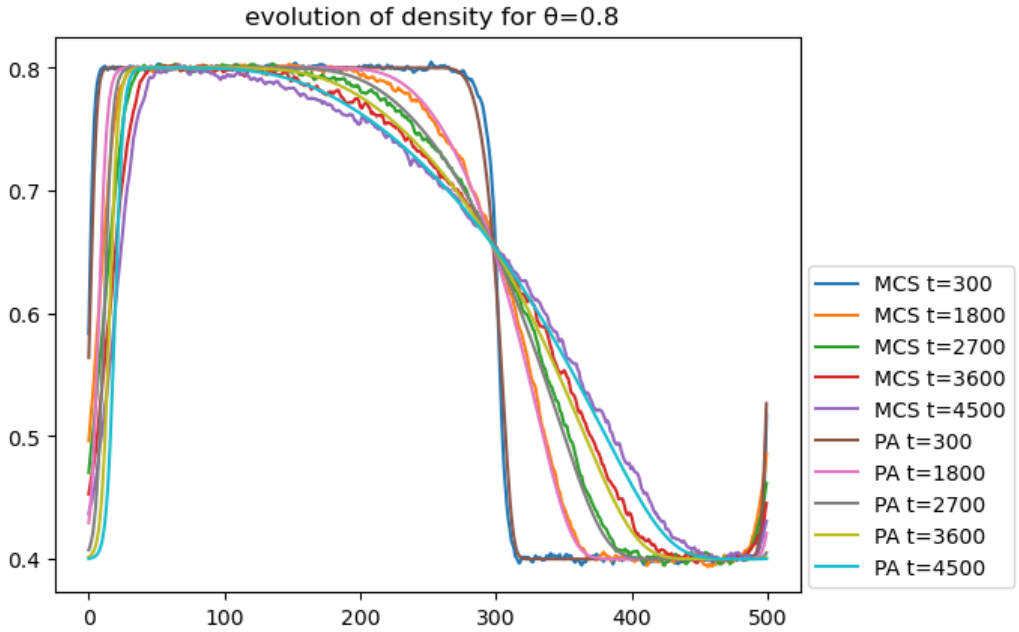

Figure 38: Same of fig. 36, but for attractive regime

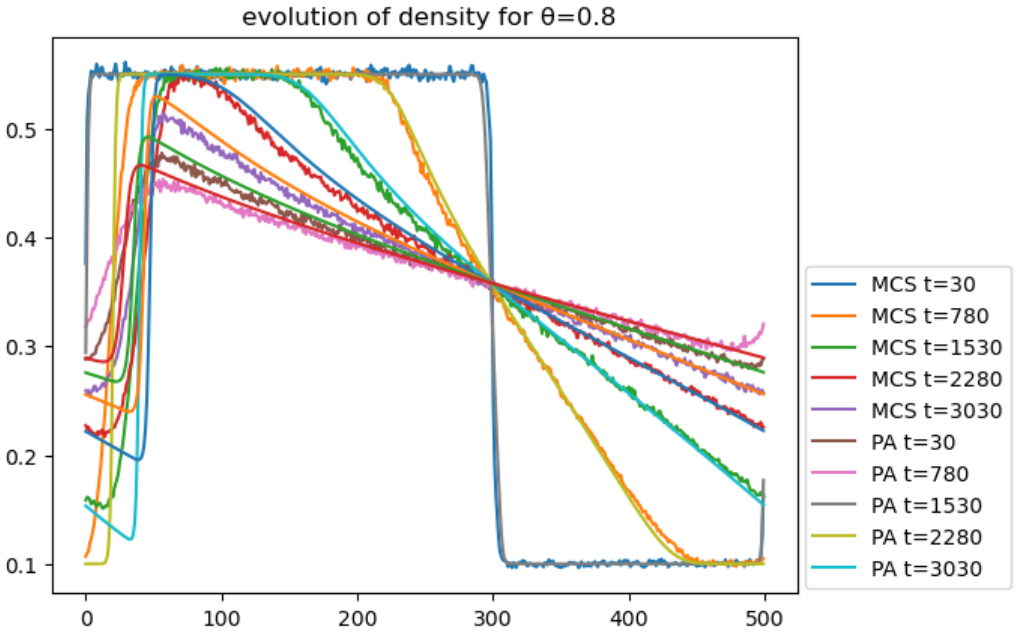

Figure 39: Time evolution of density profile for repulsive regime. We present both analytical and numerical results for different time. The smooth lines are the results of PA theory while the others are for numerical simulations.

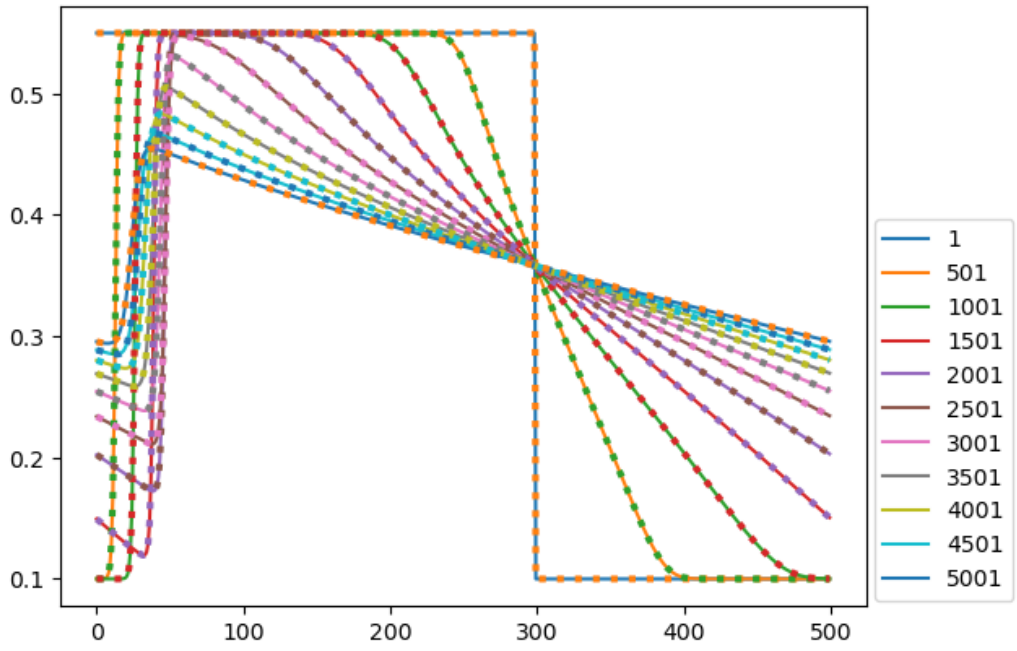

Figure 40: Comparison of the time evolutions of the density in the two model. In solid line, time evolution density of the Facilitated model with mean density $\rho = 0.63$ and repulsive regime, $\theta = 0.8$. In dot line, time evolution density of the Antal-Schütz model with mean density $\rho = 0.37$ and repulsive regime, $\theta = 0.2$.

7 Conclusions

In this thesis we have considered two different particular cases of the NN-interaction TASEP, the Facilitated Model and the Antal-Schütz model, with periodic boundary conditions, to understand both the properties of the clusters length at the steady state and the behavior of the transient from a particular initial condition to the steady state, whose properties depend on both the interaction and the mean density. The methods we have used are the Pair Approximation theory for the analytical results and the Gillespie algorithm for the numerical simulations. Concerning the probability distribution of the cluster length, we confirm the results numerically obtained in [2] for the Facilitated Model, in particular the presence of a critical density, depending on the interaction parameter, which separates a monotonic from a non-monotonic behavior, as we can see in fig. 1 and fig. 4. Using the pair approximation we have found an analytical expression for this critical density, eq. (5.1.3). Due to the particle-hole symmetry relating the Facilitated and Antal-Schütz models, this result applies also to the latter.

The other main contribution of the present work is the analysis of the transient behavior of the two models when the initial condition corresponds to a density profile with two shocks. First we concentrate our study on the Facilitated Model. The first observation is that the system takes longer times to relax to the steady state further the mean density of the system is with respect the density of maximal current. Another thing that we see is that the two shocks exists in the density profile for some times and then they meet each others, due to the fact that usually one of the two tend to diffuse while the other remains stable for a long time, this behavior is related to their velocity with respect to the group velocity of the two sides of the shock, as describe in eq. (5.2.5). Once meeting, the sharp shock continues to exist until reaching the steady state, reducing the difference of the density at the two sides, as we can see in fig. 5 and the subsequent two. After, we study the behavior of the current of the model, focusing on its dependence on the density. Within the PA theory we can find a curve in the ρ-J plane that describe the value of the current that take at the steady state depending on the density, that expression can be seen in eq. (5.2.2). Now, if we plot in the same plane, the current in function of the density at different time of the transient we can see, in fig. 21, fig. 22 and fig. 23, that they are close curve in which the current of the points on the bulks takes the values predict by the PA theory at the steady state, while the point in the sharp shock

try to mimic the curve that describe the current at the steady state, while the sharp shock connect the points in a straight line. For what concern the velocity of the shocks, it depends to both the current and the density of the two sides of them, as describe by the Rankine-Hugoniot jump condition eq. (5.2.4). Obviously this velocity can be positive (the shocks moves in the same direction of the particles) or negative (they move in the opposite direction) and this is related to the difference of the current and the density at the two sides of them.

After this, we study the Antal-Schütz model, focusing on the symmetry with the previous case, and we check that the transient behavior is similar to the one find with the Facilitated model, taking in consideration the above symmetry. Evidence of this can be seen in fig. 40.

Concerning the transient, an overall important observation is that, though not exact for this case, the PA theory style turns out to be in pretty good agreement with simulations.

References

[1] Beatrice Mina et al. "Interaction vs inhomogeneity in a periodic TASEP". In: *Journal of Physics A: Mathematical and Theoretical, Volume 57, Number 6* (2024).

[2] Quing-Yi Hao et al. "Theoretical analysis and simulation for a facilitated asymmetric exclusion process". In: *Physical Review E* (2016).

[3] Katsuiro Nishinari Andreas Schadschneider Debashish Chowdhury. *Stochastic transport in complex systems from molecules to vehicles*. Elsevier, 2011.

[4] A. Braunstein and S. Crotti. *CavityTools.jl*. Version 0.2.2. Accessed: 07/2024. 2024. URL: `https://github.com/abraunst/CavityTools.jl`.

[5] C.T. MacDonalds J.H. Gibbs and Pumpkin A.C. *Biopolymers 6,1*. 1968.

[6] C.T. MacDonald and J.H. Gibbs. *Biopolymers 7, 707*. 1969.